Workshop "Turbulence and Interface"

https://www.ercoftac.org/events/turbulence-and-interface/

Wednesday, June 15, 2022 - 9:00 - 17:00 - SkyLab, Ecole Centrale de Lyon, Ecully

8:30 - 9:00 ***Registration***

9:00 - 9:30 Welcome and opening remarks by Christophe Corre (ECL), Christophe Bailly (LMFA), Mikhael Gorokhovski (ERCOFTAC PC Henri Bénard)

9:30 - 11:15 ***Targets.*** Chair: *Claude Cambon*

9:30 - 10:00 Gholamhossein Bagheri and O. Schlenczek, B. Thiede, L. Turco, K. Stieger, J-M. Kosub, B. Hejazi, S. Clauberg, M.L. Pöhlker, Ch. Pöhlker, J. Moláček, S. Scheithauer, E. Bodenschatz, Max Planck Institute, Göttingen (Germany)
Physics of airborne disease transmission: why do we need to advance our understanding?

10:00 - 10:30 Stephane Popinet and L. Deike, W. Mostert, P. K. Farsoiya, J. Wu, B. Deremble, T. Uchida, A. Berny, T. Séon - Inst. D'Alembert, Univ. Grenoble Alpes (France), Princeton Univ. and Oxford Univ. (USA)
Toward a multiscale framework for ocean atmosphere turbulence

10:30 - 10:45 ***Refreshment Break***

10:45 - 11:15 Alain Pumir and D. Buaria - LP, Ecole Normale Supérieure Lyon (France), Max Planck Institute, Göttingen (Germany) and New York Univ., New York (USA)
Extreme events in Navier-Stokes turbulence

11:15 - 11:45 ***Turbulence and spray onset.***

Chair: *Alfredo Soldati*

11:15 - 11:45 Rodney Fox and P. K. Farsoiya, L. Deike - Iowa State Univ., Center for Multiphase Flow Research/Education and Princeton Univ. (USA)
Direct-numerical simulation of droplet breakup in homogeneous isotropic turbulence

11:45 - 12:15 Stephane Zaleski - Inst. D'Alambert, Sorbonne-Univ. (France)
Kolmogorov's and Frisch's cascade theories applied to atomization

12:30 - 13:45 ***Lunch***

13:45 - 14:15 Olivier Desjardins and L. Vu, A. Han - Cornell University (USA)
High-fidelity multi-scale modeling framework for predicting turbulent spray atomization

14:15 - 14:45 Marcus Herrmann and D. Kedelty, A. Goodrich - Arizona State Univ. (USA)
A dual scale LES model for dynamics of immiscible interfaces

14:45 - 15:15 Mikhael Gorokhovski and A. Barge, S.Oruganti - LMFA, Ecole Centrale, Lyon, LEGI, Univ. Grenoble-Alpes (France) and Argonne National Laboratory Lemont, IL 60439-4801, USA
Statistical scenarios of droplets breakup and motion in the turbulence with intermittency

15:15 - 15:30 ***Refreshment Break***

Chair: *Carlomassimo Casciola*

15:30 - 16:00 Nathanael Machicoane and O.Tolfts - LEGI, Univ. Grenoble-Alpes (France)
Statistics and dynamics of a liquid jet surrounded by a gas jet

16:00 - 16:30 Zhujun Huang and M. Alonzo, A. Cartellier - LEGI, Univ. Grenoble-Alpes (France)
Breakup of surfactant liquid jet by a coaxial airblast atomizer

16:30 - 17:00 Nicolas Rimbert and B. Ji, G. Kewalramani, Y. Dossman1, M. Gradeck, R. Meignen - Univ. Lorraine, and IRSN, Saint Paul Lez Durance (France)
Experimental Study of Liquid-liquid jet fragmentation: Eulerian and Lagrangian approach

17:00 - 17:30 Mickael Bourgoin and T. Basset, B. Viggiano, T. Barois, M. Gibert, N. Mordant, R. B. Cal, R. Volk - LP, Ecole Normale Supérieure de Lyon (France) and LEGI, Univ. Grenoble-Alpes (France)
Entrainment, diffusion and effective compressibility in a self-similar free shear turbulent jet

17:30 ***Welcome aperitif***

---------- ***end of the first day*** ----------

Thursday, June 16, 2022 - 9:00 - 11:45 - SkyLab, Ecole Centrale de Lyon, Ecully

Interface dynamics at a high and a low Reynolds numbers. External intermittency.

Chair: *Mickael Bourgoin*

9:00 - 9:30 Filippo Coletti - ETH, Zurich (Switzerland)
Spatial and Temporal Scales of Free-Surface Turbulence

9:30 - 10:00 Luminita Danaila and Zh. Zhang, I. Danaila, E. Levéque - Univ. Rouen and LMFA, Ecole Centrale de Lyon (France)
High-order statistics and intermittency of a two-fluid HVBK quantum turbulent flow

10:00 - 10:30 John-Christos Vassilicos - LMFL, Centrale Lille, Univ. Lille (France)
The energy cascade at the turbulent/non-turbulent interface

10:30 - 10:45 ***Refreshment Break***

10:45 - 11:15 Sergio Chibbaro and M. C. Esposito, L. Brandt - Univ. Paris-Saclay (France) and KTH Royal Institute of Technology (Sweden)
Modulation of homogeneous and isotropic turbulence in emulsions

11:15 - 11:45 Maria Vittoria Salvetti and A. Mariotti, M. Antognoli, S. Tomasi Masoni, E. Brunazzi, C. Galletti, R. Mauri - Univ. Pisa (Italy)
Fascinating interface topology and dynamics in micro mixers

12:00 - 12:45 ***Lunch***

13:00 - Workshop will move for an afternoon session to Maison d'Ampère in Poleymieux-au-Mont-d'Or, including visit of the Museum – Historic Site of European Physics

Thursday, June 16, 2022 - 14:00-18:30, Maison d'Ampère, Poleymieux-au-Mont-d'Or

13:45 - 14:00 Words of Welcome by Genevieve Comte-Bellot

Turbulence ⇔ Particles.

Chair: *Rodney Fox*

14:00 - 14:30 Carlomassimo Casciola and F. Seraffni, F. Battista, P. Gualtieri - Sapienza Univ. Rome (Italy)
Drag reduction in turbulent pipe flows of realistic polymer solutions

14:30 - 15:00 Olivier Simonin and A. Boutsikakis, P. Fede - IMFT, Univ. Toulouse (France)
On the modelling and simulation of the dynamic of charged particles in turbulent flow

15:00 - 15:30 Gautier Verhille and B. Favier, P. Le Gal - IRPHE, Aix-Marseille Univ. Centrale Marseille (France)
Inertial deformable particles in turbulence

15:30 - 15:45 ***Refreshment Break***

Chair: *Olivier Desjardins*

15:45 - 16:15 Alfredo Soldati and F. Mangani1, A. Roccon - TU Wien, Vienna (Austria) and Univ. Udine (Italy)
Influence of density and viscosity on deformation, breakage and coalescence of bubbles in turbulence

16:15 - 16:45 Frederic Risso and F. Le Roy de Bonneville, R. Zamansky, A. Boulin, J.-F. Haquet - IMFT, Univ.Toulouse and CEA, Saint-Paul-Lez-Durance (France)
Dynamics of bubble-induced turbulence from coarse-grained simulations

16:45 - 17:15 Kai Schneider - Centre de Mathematiques et d'Informatique, Aix-Marseille Univ. (France)
Multiscale techniques for analyzing voids and clusters in particle-laden turbulence

17:15 - 18:00 ***Guided Tour of Museum***

18:00 - ***Bus to Lyon Center (place Bellecour, Lyon 69002)***

19:30 - ***Social Diner in Brasserie Georges–1836, Lyon (30 cours de Verdun, 69002, Lyon)***

---------- end of the second day ----------

Friday, June 17, 2022 - 9:00-17:00 - SkyLab, Ecole Centrale de Lyon, Ecully

Turbulence, Particles, Scalars

Chair: *Emmanuel Lévèque*

9:00 - 9:30 Sander Huisman and S. Angriman, P. Cobelli, M.Bourgoin, R. Volk, P.Mininni, Max Planck UT Center (Germany) Univ. Twente (Netherlands), LP, ENS (France) and Univ. Buenos Aires (Argentine)
Broken mirror symmetry of tracer's trajectories in turbulence

9:30 - 10:00 Herman Clercx and M. Madonia, A. A. Guzmán, X. de Wit, R. Kunnen - Eindhoven Univ. of Technology, Eindhoven (Netherlands)
Turbulent rotating Rayleigh-Bénard convection: Flow organization and heat transfer in slender confined cylinders

10:00 - 10:30 Martin Obligado and A. Ferran, N. Machicoane, N. Mordant, A. Aliseda - LEGI, Univ. Grenoble Alpes, Grenoble (France) and Univ. Washington, Seattle (USA)
Gravitational settling of inertial particles in homogeneous isotropic turbulence

10:30 - 10:45 ***Refreshment Break***

Chair: *Olivier Simonin*

10:45 - 11:15 Cristian Marchioli and A. Hajisharifi1, A. Soldati - Univ. Udine (Italy) and TU Wien (Austria)
Particle capture by large deformable drops in turbulent flow

11:15 - 11:45 Francesco Picano and J. Wang, F. Dalla Barba - Univ; Padova (Italy)
On the evaporation of dilute droplets in turbulent jets: from physics to applications

11:45 - 12:15 Aurore Naso and M. Z. Sheikh, K. Gustavsson, E. Lévêque, B. Mehlig, A. Pumir - LMFA, Ecole Centrale Lyon and LP, Ecole Normale Supérieure de Lyon (France)
Collisions between ice crystals in clouds

12:15 - 12:45 Loïc Méès and N. Grosjean, and J. L. Marie - LMFA, ECL (France)
Lagrangian tracking of evaporating droplets in a homogeneous quasiisotropic turbulence

12:45 - 13:15 Daniela Tordella and L. Fossa, Sh. Abdunabiev, M. Golshan - Politechnico Turin (Italy)
Microphysical time scales and local supersaturation balance at a warm Cloud Top Boundary

13:15 - 14:00 ***Lunch and Concluding remarks*** by Alfredo Soldati, Mickael Bourgoin and Mikhael Gorokhovski

---------- ***end of the third day*** ----------

Physics of airborne disease transmission: why do we need to advance our understanding?

Gholamhossein Bagheri, Oliver Schlenczek, Birte Thiede, Laura Turco, Katja Stieger, Jana-Michelle Kosub, B. Hejazi, Sigrid Clauberg, Mira L. Pöhlker, Christopher Pöhlker, Jan Moláček, Simone Scheithauer, Eberhard Bodenschatz

Max Planck Institute, Göttingen (Germany)

COVID-19 and other airborne diseases are transmitted to healthy individuals through the inhalation of pathogen-containing particles exhaled by infectious individuals. I will provide an overview of the mechanisms involved in the formation of these particles and the effects of social distancing and masking on transmission risk. I will present the results of our experimental study to characterize the size distribution of exhaled particles from more than 130 individuals aged 5 to 80 years using aerosol size spectrometers and in-line holography. In total, we collected and analyzed exhaled samples for 100 hours using the spectrometers and 12000 holograms. The respiratory maneuvers studied are mouth/nose breathing, loud/normal speaking, singing, humming, shouting, coughing, and playing wind instruments. Using these results, the physical basis of exhalation flow, leakage from face masks of various types and fits measured in human subjects, consideration of particle shrinkage in the environment due to evaporation, and rehydration, inhalability, and deposition in the susceptible airways, the upper limit of infection with SARS-CoV-2 for one-to-one exposure is calculated. I will show that wearing appropriate masks in the community provides excellent protection for others and oneself and makes social distancing less important.

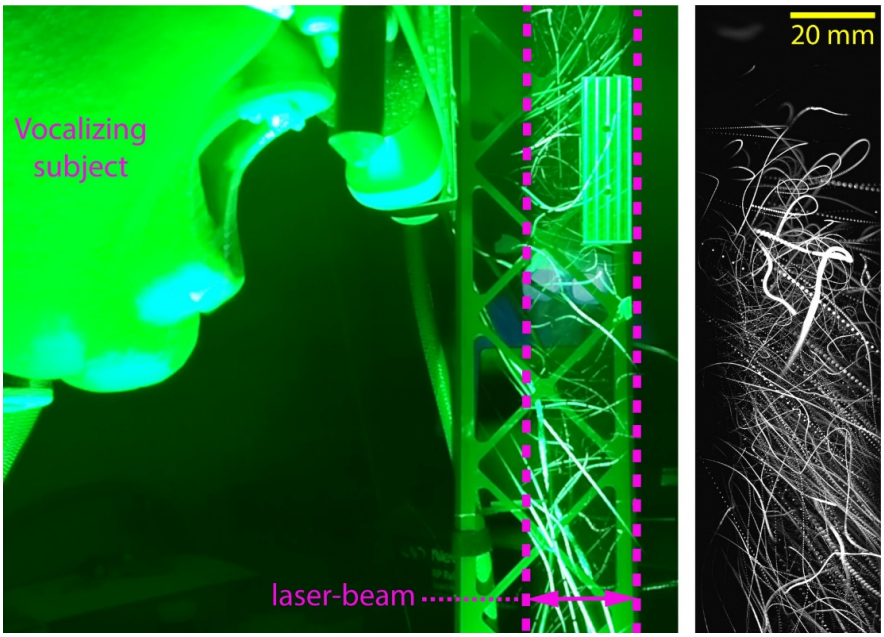

Toward a multiscale framework for ocean–atmosphere turbulence

BY S. POPINET[1], L. DEIKE[2], W. MOSTERT[2,3], P. K. FARSOIYA[2], J. WU[2], B. DEREMBLE[4], T. UCHIDA[4], A. BERNY[1], T. SÉON[1]

[1] Institut Jean le Rond ∂'Alembert, [2] Princeton University, [3] Oxford University, [4] Université Grenoble Alpes

Turbulent exchanges of mass, heat and momentum between the ocean and the atmosphere are a critical component of the climate system. Climate models currently use relatively crude semi-empirical parameterisations of these fluxes often based on in-situ observation campaigns. The limitations of these parameterisations (range of validity, robustness, sensitivity etc.) are well-known to climate modellers. They are due both to the difficulty of acquiring enough experimental data and to a lack of understanding of the complex processes linking sub-millimetric physics to kilometre-scale fluxes. In this talk, I will report on recent results from a collaborative effort to build a hierarchy of theoretical and numerical models able to span this range of spatial scales. The resulting framework will hopefully allow to fill the gap in available experimental/field data and to make the link between climate-scale parameterisations and small-scale physics.

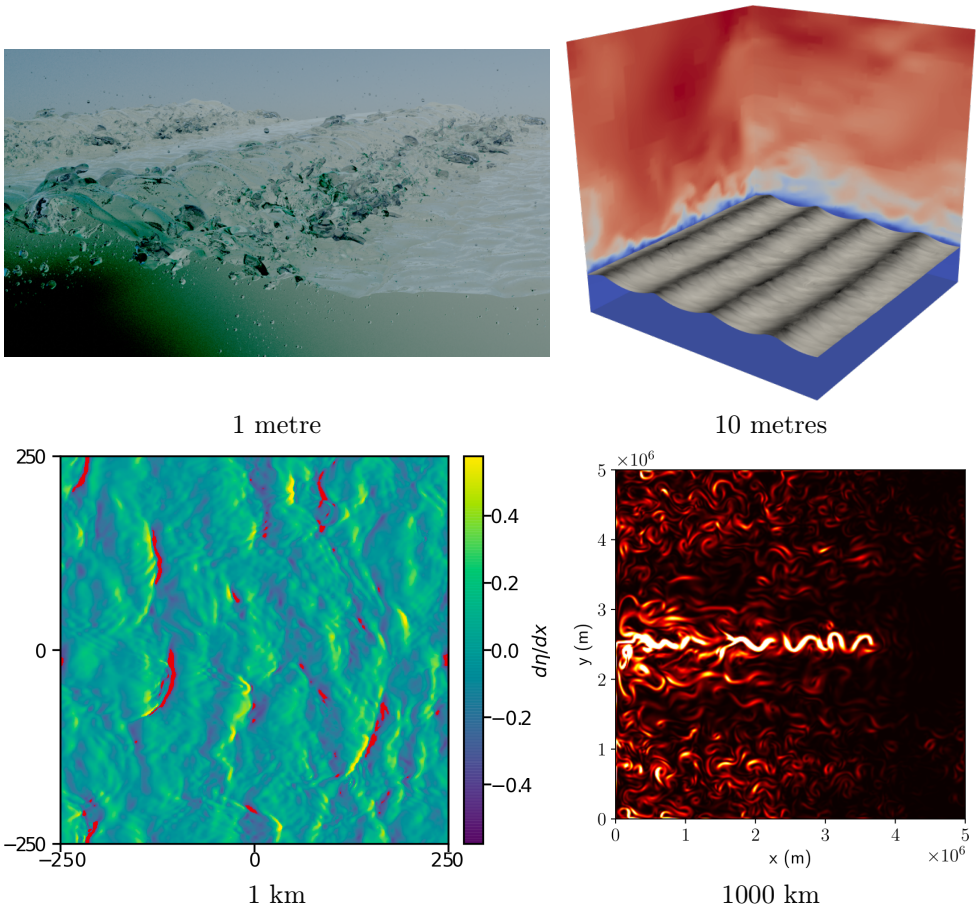

Figure 1. (top left) Direct Numerical Simulation of wave breaking [1]. (top right) Interaction between a wave field and a turbulent atmospheric boundary layer [2]. (bottom left) Distribution of breaking events for a realistic oceanic wave spectrum [3]. (bottom right) Eddy kinetic energy for a quasi-geostrophic mid-latitude ocean model [4].

References

[1] W. Mostert, S. Popinet, and L. Deike. High-resolution direct simulation of deep-water breaking waves: transition to turbulence, bubbles and droplets production. *Journal of Fluid Mechanics*, in press, 2022.

[2] J. Wu, S. Popinet, and L. Deike. Revisiting wind wave growth with fully-coupled direct numerical simulations. Submitted to *Journal of Fluid Mechanics*, 2022.

[3] S. Popinet. A vertically-Lagrangian, non-hydrostatic, multilayer model for multiscale free-surface flows. *Journal of Computational Physics*, 418:109609, 2020.

[4] T. Uchida, B. Deremble, and S. Popinet. Deterministic model of the eddy dynamics for a midlatitude ocean model. *Journal of Physical Oceanography*, in press, 2022.

EXTREME EVENTS IN NAVIER-STOKES TURBULENCE

Alain Pumir[1,2] & Dhawal Buaria[3,2]
[1]*Laboratoire de Physique, Ecole Normale Supérieure de Lyon and CNRS, Lyon, France*
[2]*Max Planck Institute for Dynamics and Self-Organization, Göttingen, Germany*
[3]*Tandon School of Engineering, New York University, New York, USA*

The spotaneous and intermittent generation of very intense velocity gradients is a defining property of fluid turbulence [1, 2]. We investigate here the fundamental question: how large can these extreme fluctuations be ? To this end, we utilize data from direct numerical simulations of isotropic turbulence in periodic domains, with very high spatial and temporal resolution at Reynolds number R_λ in the range $140 - 1300$ [2, 3], with up to 18432^3 grid points. As a manifestation of intermittency, the probability density function (PDF) of the enstrophy, $\Omega \equiv |\omega|^2$, where ω is vorticity, divided by its mean, τ_K^{-2}, where $\tau_K = \langle\Omega\rangle^{-1/2}$, develops tails which reach increasingly large values when R_λ increases. Remarkably, the tails of these distributions can be collapsed by scaling Ω by τ_{ext}^{-2}, with $\tau_{ext} = \tau_K \times R_\lambda^{-\beta}$, with $\beta < 1$, see Fig. 1a.
Regions where Ω is most intense have the shape of vortex tubes, which can be assumed to be Burgers-like vortices. Their size results from a balance between viscosity, ν, which broadens the vortex tube, and some effective strain rate, S_e, which stretches the vortex along the direction of the tube, leading to a radius $\sim (\nu/S_e)^{1/2}$.
To estimate the effective strain acting on intense vortices, we condition $\Sigma \equiv 2\mathrm{tr}(\mathbf{S}^2)$, where $\mathbf{S}$ is the strain-rate tensor, on enstrophy. Remarkably, Fig. 1b shows that $\langle\Sigma|\Omega\rangle \sim \Omega^\gamma$, where γ is an exponent smaller than 1, increasing slowly with R_λ. To estimate the characteristic scale of the vortices we estimate the external strain, S_e, acting vortices of enstrophy Ω, as $\langle\Sigma|\Omega\rangle^{1/2}$. We also use the observation that the velocity increments across intense vortex tubes are of the order of the *r.m.s.* of the velocity fluctuations in the flow [2]. These observations lead to the relation $\beta = 1/(2-\gamma)$, consistent with the measured values of β and γ.
The dependence of γ on R_λ, shown in Fig. 1b, can be fitted by $\gamma = 1 - pR_\lambda^{-q}$ ($\ln p = -0.033$ and $q = 0.189$). It implies that the exponent β in fact depends on R_λ. To study quantitatively this dependence, we use the observation that the large tails of the PDFs of Ω can be represented to a very good accuracy by a stretched exponential, of the form $P(\Omega) = a\exp(-b\Omega^c)$ [2, 3]. We fitted the tails of the PDF of Ω, assuming various values of the exponent c, see Fig. 1c. The scaling for the extreme events of Ω is consistent with the stretched exponential form of $P(\Omega)$ provided: $d\ln(b^{1/c})/d\ln(R_\lambda) = -2/(2-\gamma)$. Using the dependence of γ on R_λ leads to the dashed lines in Fig. 1c. The symbols shown on the graphs, corresponding to the fits of the PDF of Ω, agree very well with our prediction (see the dashed line).

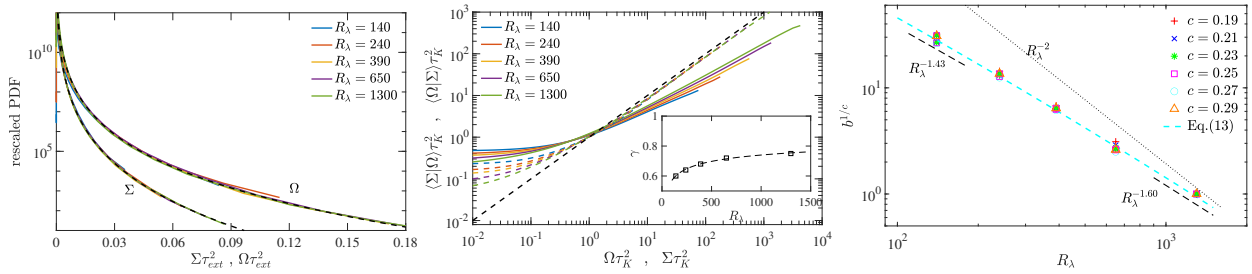

Figure 1. a, left: Superposition of the PDF of Ω, divided by $\tau_{ext}^2 \equiv \tau_K^2 R_\lambda^{-2\beta}$. b, center: The dependence of $\langle\Omega|\Sigma\rangle$ (dashed lines), and of $\langle\Sigma|\Omega\rangle$ (full lines), which can be represented by a power law, $\langle\Sigma|\Omega\rangle \sim \Omega^\gamma$. The dependence of the exponent γ on R_λ is shown in the inset. c, right: The dependence of the coefficient b obtained by fitting the PDF of Ω by a stretched exponential form, $P(\Omega) = a\exp(-b\Omega^c)$ with an exponent c close to $1/4$. The dashed lines, obtained from the fitted dependence of γ on R_λ, accurately captures the data points.

In the limit $R_\lambda \to \infty$, we expect $\gamma, \beta \to 1$, which corresponds to the prevailing intermittency theories [3]. Our results however, indicate that this asymptotic regime is reached only at extremely large Reynolds number, unrealizable on Earth. The difference between our approach and classical intermittency theory comes from estimating the vortex size using the simplified structure of Burgers vortices, controlled by the local strain. This indicates that understanding the strain, and in particular the exponent γ, is a major theoretical challenge to describe extreme events in turbulence.

References

[1] U. Frisch. Turubulence: the legacy of A. N. Kolmogorov, *Cambridge University Press* 1995.
[2] D. Buaria, A. Pumir, E. Bodenschatz, and P. K. Yeung, *New J. Phys.* **21**:043004, 2019.
[3] D. Buaria and A. Pumir, *Phys. Rev. Lett.* **128**:194501, 2022.

Direct-numerical simulation of droplet breakup in homogeneous isotropic turbulence

P. K. Farsoiya[1,2], L. Deike[1,2], and R. O. Fox[3,4]
[1] Dept. of of Mechanical and Aerospace Engineering, Princeton University, USA
[2] High Meadows Environmental Institute, Princeton University, USA
[3] Dept. of Chemical and Biological Engineering, Iowa State University, USA
[4] Center for Multiphase Flow Research and Education, ISU, USA

Following the methodology developed for bubbles by Riviere et al. (2021), we investigate the break up of an immiscible liquid droplet in homogeneous isotropic turbulence (HIT) of a continuous liquid. Direct-numerical simulations are performed with the Basilisk software (Popinet, 2009) for Newtonian fluids with different densities (ρ_d, ρ_c), viscosities (μ_d, μ_c), and surface tension (γ). A spherical droplet of diameter d is placed in fully developed HIT for fixed Taylor-scale Reynolds number Re_λ and followed until break-up. A systematic investigation varying the Weber number and the Ohnesorge number $\mathrm{Oh} = \mu_d/\sqrt{\rho_d \gamma d}$ (Hinze, 1955) has been carried out. Of particular interest for model development are the breakage frequency and the child size distribution, and their dependence on the dimensionless numbers.

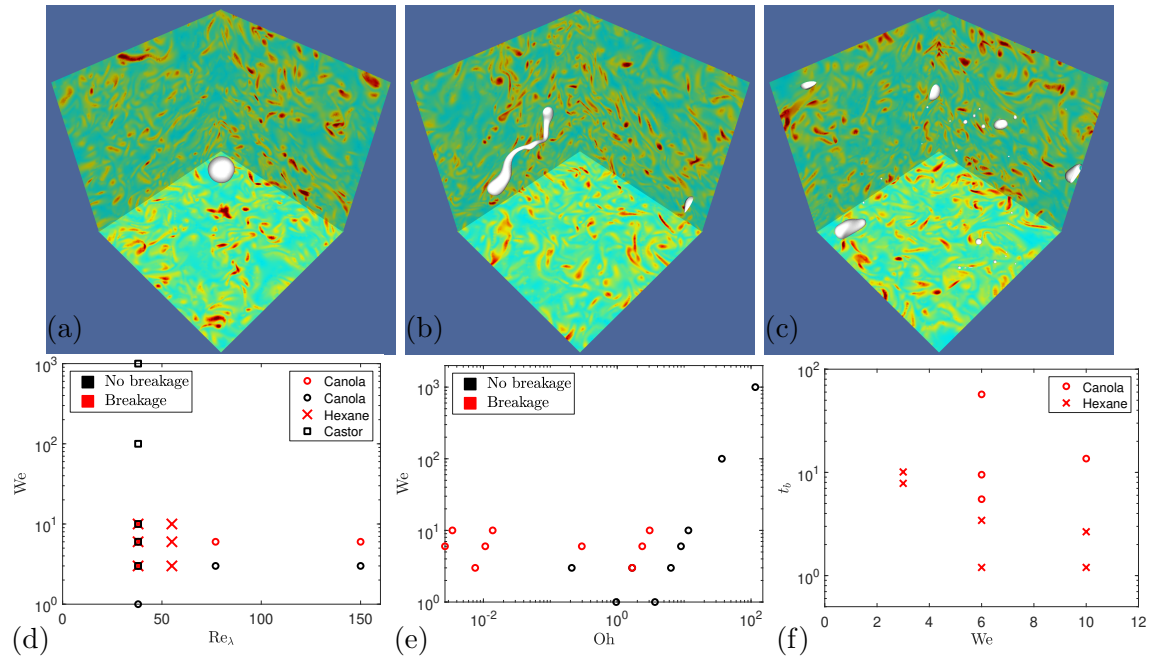

Figure 1: Droplet in HIT flow: (a) $t/t_c = 0$, (b) $t/t_c = 9$, (c) $t/t_c = 12$. Characterization of droplet breakup: (d) $\mathrm{Re}_\lambda - \mathrm{We}$, (e) $\mathrm{Oh} - \mathrm{We}$, (f) time for first breakup $\mathrm{We} - t_b$.

References

A. Rivière, W. Mostert, S. Perrard, and L. Deike. *Sub-Hinze scale bubble production in turbulent bubble break-up.* J. Fluid Mech., **917**, A40, 2021.

S. Popinet. *An accurate adaptive solver for surface-tension-driven interfacial flows.* J. Comp. Physics., **228**, 5838–5866, 2009.

J. O. Hinze. *Fundamentals of the hydrodynamic mechanism of splitting in dispersion processes.* AIChE J., **1**, 289–295, 1955.

Kolmogorov's and Frisch's cascade theories applied to atomization

Stephane Zaleski

abstract: Many experiments and simulations of atomization show either a Log-Normal particle size probability density function (PDF) or a Pareto one, including, strikingly, in human exhalation aerosol studies going back to the first part ot the 20th century. The theory of Kolmogorov is exceedingly simple and leads naturally to a Log-Normal distribution, and was indeed applied to fragmentation. The beta model, Frisch, Sulem and Nelkin's cascade theory, can be seen as a singular perturbation of the Log-Normal theory for single phase turbulence and leads naturally to Pareto, in this context called fractal, models. It is easy to generalize the beta model to flows with interfaces, leading to scaling theories for the sheets, ligaments and droplets of atomization.

High-fidelity multi-scale modeling framework for predicting turbulent spray atomization

L. Vu, A. Han, and O. Desjardins
Sibley School of Mechanical and Aerospace Engineering, Cornell University

The computational prediction of turbulent liquid atomization presents enormous challenges, in part because of the wide range of length and time scales involved in the spray break-up process. While direct numerical simulation (DNS) approaches have been increasingly applied to the study of liquid-gas flows in recent years, their computational cost is typically too large to enable the prediction of spray properties under realistic flow conditions. Large-eddy simulation (LES) approaches have the potential to be much cheaper, but their application to liquid atomization has remained difficult.

In this work, we propose to tackle the challenge of LES of liquid atomization with a novel multi-scale modeling framework wherein multiple computational domains are interfaced, with each domain tackling a different length scale of the spray atomization problem. Upstream, we simulate the internal gas flow of the nozzle using a single-phase LES. This generates the gas inflow conditions for a volume-of-fluid (VOF) LES of the spray formation region. Thanks to a two-plane liquid-gas interface reconstruction, small interfacial features such as sheets and ligaments can be represented conservatively at the sub-grid scale. A connected component labeling algorithm analyses the Eulerian field on the fly and identifies sheets and ligaments as Lagrangian objects, which can then be fed as input to various physics-informed break-up models. Here, a simple break-up model applicable to both ligaments and sheets is introduced. The Lagrangian drops generated by this break-up model are evolved in an Euler-Lagrange LES performed on a much larger domain, wherein turbulent spray dispersion is simulated. We demonstrate the effectiveness of the methodology by comparing a simulation of turbulent airblast atomization to experimental data such as effective liquid path length, liquid core length, flapping frequency, but also droplet size distribution, showing favorable agreement for all metrics.

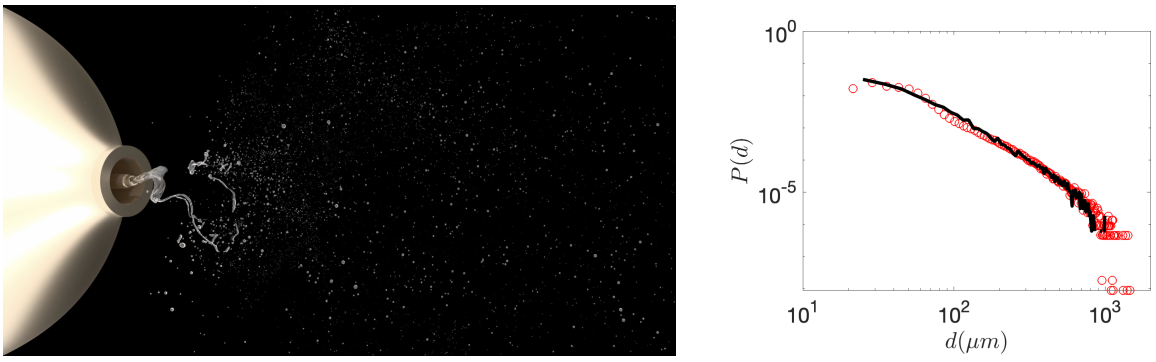

Figure 1: Left: snapshot of the liquid-gas interface in a simulation of airblast atomization. Right: comparison between droplet size distribution from simulation (line) and experiments (symbols).

A dual scale LES model for dynamics of immiscible interfaces

D. Kedelty, A. Goodrich, and M. Herrmann
School for Engineering of Matter, Transport and Energy, Arizona State University

While significant progress has been made in the past decade to predict atomization using detailed numerical simulations, these come at significant computational cost since the range of scales that must be resolved exceeds those of a single phase turbulent flow significantly. A switch to a Large Eddy Simulation (LES) approach would be desirable, however, the underlying assumption of LES methods that the dynamics of the unresolved sub-filter scale can be inferred from the resolved scales is questionable when atomization occurs. Similar to viscosity in single-phase flows, surface tension scales with the inverse of a length-scale, but unlike viscosity, it can act to either dissipate surface corrugations preventing breakup, giving rise to Kolmogorov's critical radius (Hinze scale), or enhance surface corrugations due to the Rayleigh-Plateau instability, resulting in breakup. Which process is dominant on the sub-filter scale seems to depend entirely on the sub-filter interfacial geometry, i.e., if the interface is in the shape of ligaments, the surface tension can lead to breakup, whereas in other cases, surface-tension forces can inhibit breakup. Unfortunately, the sub-filter geometry cannot be inferred from the filtered interfacial geometry alone. LES approaches going beyond the traditional single-phase cascade hypothesis may be required for two-phase flows with atomization.

In this presentation, a dual scale LES modeling approach will be discussed that can handle the dual nature of surface tension on the sub-filter scale. The model maintains a fully resolved realization of the phase interface, shifting the modeling task to reconstructing the fully resolved interfacial advection velocity from the filter-scale velocity, taking the effects of sub-filter surface tension, turbulent eddies, shear, and acceleration into account. Results showing the viability of the dual-scale LES approach in canonical test cases including initially planar surfaces and sheets in turbulent flow fields will be discussed.

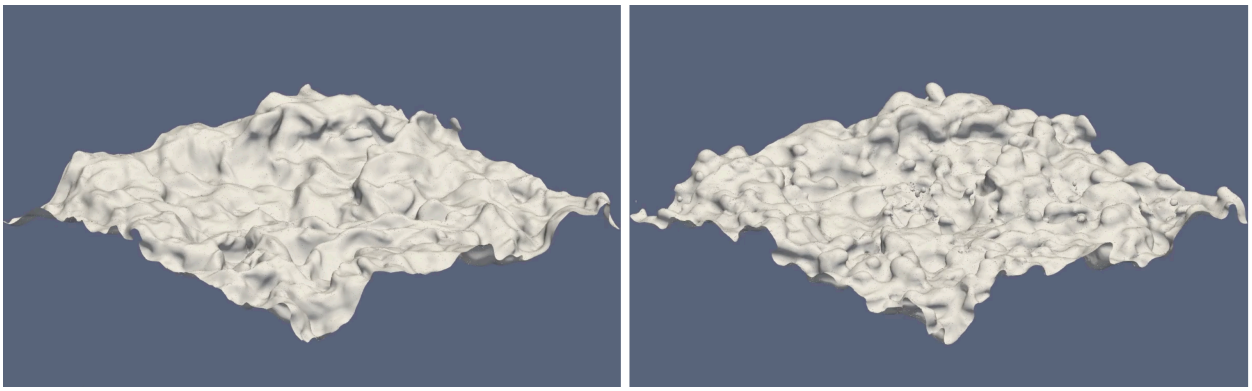

Figure 1: DNS (left) and Dual Scale LES realization of an initially planar interface in decaying homogeneous isotropic turbulence at $t/t_\lambda = 0.1$ *with* $Re_\lambda = 156$ *and* $We_\lambda = 1.1$.

*Supported by NSF-CBET-1803657 and NASA's NNX16AB07A.

Statistical scenarios of droplets breakup and motion in the turbulence with intermittency

M. Gorokhovski[1], A. Barge[2] and S. Oruganti[3]
[1] LMFA, Ecole Centrale de Lyon, 69134 Ecully, France
[2] Univ. Grenoble Alpes, CNRS, Grenoble INP, LEGI, 38000 Grenoble, France
[3] Argonne National Laboratory Lemont, IL 60439-4801, USA

The highly intermittent flow structure in turbulence at the high Reynolds number (see [1], for example, where the extreme increments of the velocity are characterized by smallest scales, even less that the Kolmogorov one) raise a question of how to introduce the intermittency effects in the stochastic scenario of spray formation and dispersion.
In the first part of this talk we are focused on the statistical physics of droplet breakup process.
We considered two approaches. The first one is based on the stochastic relaxation of droplet size to its expected maximum stable value. For the latter, in contrast to the Kolmogorov-Hinze critical size, our expression contains the droplet inertia, as a breakup parameter of the selective response to turbulent disruptive forces [2]; concomitantly, the relaxation to this size, includes the intermittency effects. The second statistical breakup model is based on the fragmentation theory with the fragmentation frequency decreasing with the droplet size. In this case, we will show that considering the fragmentation equation in the continuity form [3], the self-similar solution (or intermediate asymptotics) for the size distribution takes the form of the well-known Nukiyama–Tanasawa distribution. The latter is controlled by the viscous dissipation rate. We will also show the conditions in which that intermediate asymptotic may take the lognormal and then the Pareto-type forms.
In the second part of this talk we will present the modified stochastic equations of the point-wise droplets with size above and below the dissipative Kolmogorov length-scale. The main role in those equations is devoted to two parameters "seen" by a droplet. The first is the norm of the fluid particle acceleration, and the second is its orientation. Both are simulated as stochastic processes. With increased local Reynolds number, these models give more stretched tails in the droplets acceleration distribution, thereby the autocorrelation time of the droplet acceleration is increased as well [4-6]. We will show the new comparisons between these models and predictions from DNS.

References

1. D. Buaria, A. Pumir, E. Bodenschatz and P.K. Yeung. New J. Phys. 21 043004, 2019
2. M. Gorokhovski, Atomization and Sprays, 11, 505-519, 2001
3. V.L. Saveliev and M.A. Gorokhovski, Phys. Rev. E. 061112, 11, 2012
4. M. Gorokhovski and R. Zamansky. Phys. Rev. Fluids 3, 034602, 2018
5. A. Barge and M. Gorokhovski. J. Fluid Mech. vol. 892, A28, 2020
6. M. Gorokhovski, S. Oruganti. J. Fluid Mech. vol. 932, A18, 2022

Statistics and dynamics of a liquid jet surrounded by a gas jet

O. Tolfts[1], N. Machicoane[1]
[1] Univ. Grenoble Alpes, CNRS, Grenoble INP, LEGI, 38000 Grenoble, France

The destabilization of a liquid jet into a spray by a surrounding gas jet is a process that is often used in applications such as manufacturing, combustion, or fire safety. This phenomenon is thoroughly studied in the context of coaxial two-fluid atomization. Close to the atomizer exit, the stresses imposed by the gas flow deform the liquid jet, leading to its fragmentation. A first-glance large-scale metric consists of the liquid core length, corresponding to the extent of the liquid jet that is still connected to the atomizer. This metric was studied early on and has proven relevant for applications and modeling purposes. While scaling laws of the liquid core length along variations of the spray operating parameters were widely proposed, past studies focused solely on its average value, despite the turbulent nature of the two-phase flow forming the spray, ignoring higher order statistical moments and the temporal dynamics of the liquid jet.

We present an experimental study of coaxial two-fluid atomization using high spatial and temporal resolution back-lit imaging and study the statistics and dynamics of the liquid core length. We show that the statistics are non-Gaussian, and are solely driven by one parameter, the gas-to-liquid dynamic pressure ratio M (Fig. 1). We also propose a parametric expression that collapses all experimental distributions onto two master curves. The master curves differ only from their third order moment and are separated by a threshold in the gas Reynolds number. In addition, the liquid core length timescales are found to be mostly driven by the turbulent gas jet, with a secondary weak dependency on the liquid Reynolds number.

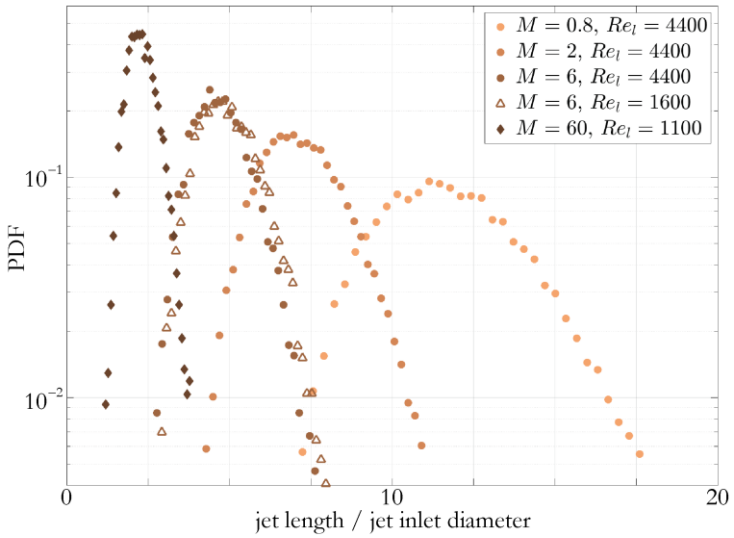

Figure 1: Probability density functions (PDF) of the liquid core lengths for different spray conditions spanning laminar and turbulent liquid jets. The values of the liquid Reynolds number Re_l and gas-to-liquid dynamic pressure ratio M are indicated.

Breakup of surfactant liquid jet by a coaxial airblast atomizer

M. Alonzo, Z. Huang*, and A. Cartellier
Univ. Grenoble Alpes, CNRS, Grenoble INP, LEGI, 38000 Grenoble, France

The mechanisms that affect breakup liquid jet into droplets by atomisation have been widely studied [1]. However in many technological and natural processes, the liquid jet may contains surfactant solutions under nonequilibrium conditions. Few researches addressed this topic for the spray [2, 3]. The role of surfactants on the breakup of liquid jet surrounded by a coaxial air flow has been examined in this study over a wide ranges of water and air jet flow ($U_L = 0.1 - 0.3m/S$, $U_G = 23 - 57m/S$). Three surfactants (SDS, $C_{12}TAB$, $C_{16}TAB$) have been used at different concentrations, which allowed to explore a range of characteristic time for adsorption varying from 1 ms to 1 s. The images obtained by high-speed camera show that the surfactants don't change the frequency of the shear and flapping instability. However, those with fast adsorption kinetics may reduce quickly the surface tension at the end of the liquid jet before its breakup, therefore increase significantly the breakup length (Fig.1a). The presence of these surfactants in the water reduce also the oscillation amplitude of liquid jet and the breakup frequency. At a low air injection velocity, the change of breakup regime from fiber/ligament to membrane dominant has been observed (Fig.1b and 1c). The droplets size in the spray have been investigated by a combination of phase detection optical probes and laser diffraction. Results show that the surfactants not only leads to a small decrease of the mean droplet size, but also modified the droplet size distributions of spray. Methodological details and mechanism that determine the droplet size distribution will be discussed in the oral presentation.

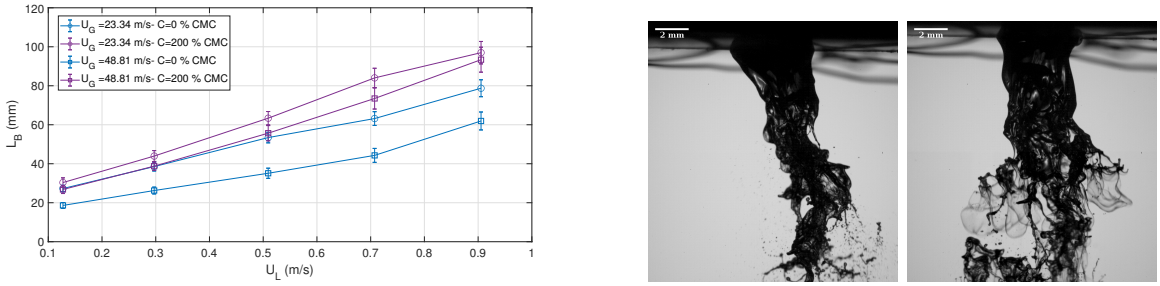

(a) (b) (c)

Figure 1: Effect of surfactant $C_{12}TAB$ on the mean breakup length (a) and breakup regime. High-speed photographs of the breakup process: (b) water and (c) water with $C_{12}TAB$ at 2× CMC. The formation of bags are clearly visible in the latter case.

References

[1] J. C. Lasheras, E. Villermaux, and E. J. Hopfinger. Break-up and atomization of a round water jet by a high-speed annular air jet. *Journal of Fluid Mechanics*, 357:351–379, 1998.

[2] U. Shavit and N. Chigier. The role of dynamic surface tension in air assist atomization. *Physics of Fluids*, 7(1):24–33, 1995.

[3] R. Sijs, S. Kooij, and D. Bonn. How surfactants influence the drop size in sprays from flat fan and hollow cone nozzles. *Physics of Fluids*, 33(11):113608, 2021.

*Corresponding Author: zhujun.huang@univ-grenoble-alpes.fr

Experimental Study of Liquid-liquid jet fragmentation: Eulerian and Lagrangian approach

Nicolas Rimbert[1], Bowen Ji[1], Gagan Kewalramani[1], Yvan Dossman[1], Michel Gradeck[1], Renaud Meignen[2]
[1] *LEMTA, CNRS Université de Lorraine, Vandœuvre-lès-Nancy, 54518, France,*
[2] *Institut de Radioprotection et de Sûreté Nucléaire (IRSN) Saint Paul Lez Durance, 13115,France.*

Topic(s): Lagrangian and Eulerian approaches for particulate flows

Abstract:

In order to understand fundamentals of liquid-liquid jet breakup, a jet of Cargille laser fluid (density 1896kg/m^3, viscosity 26 mPa.s, surface tension to water 0.0265 Nm^{-1}) injected into a water pool is studied. The Cargille fluid has been purchased so that it matches water refractive index at 20°C (n = 1.3330). A laser sheet (532nm wavelength) is then used and Pyrromethene 597 is used as fluorescent dye to trace Cargille fluid location otherwise undistinguishable from water. A high-speed camera (phantom V710) is used to record the experiments. Data (cf. figure 1) are then processed using a Lagrangian tracking algorithm (based on Kalman filtering) showing the birthplace of elementary droplet related to primary fragmentation of the jet. The postprocessing also allows to put secondary fragmentation and collision into evidence when they happen inside the light sheet. To understand the size of the droplet produced by primary fragmentation, a Eulerian dynamic mode decomposition algorithm [1] is used to study instabilities that are localized in the near nozzle area (see red box on figure 2) of the jet. Results shows that for resolved droplet, instability wavelength correlates with the size of the droplets and that Entov-Yarin [2] (longwave) bending instability plays an important role albeit most classical instability modes (Sterling-Sleicher [3], Lin & Reitz [4], Rayleigh…etc.) seem to be present.

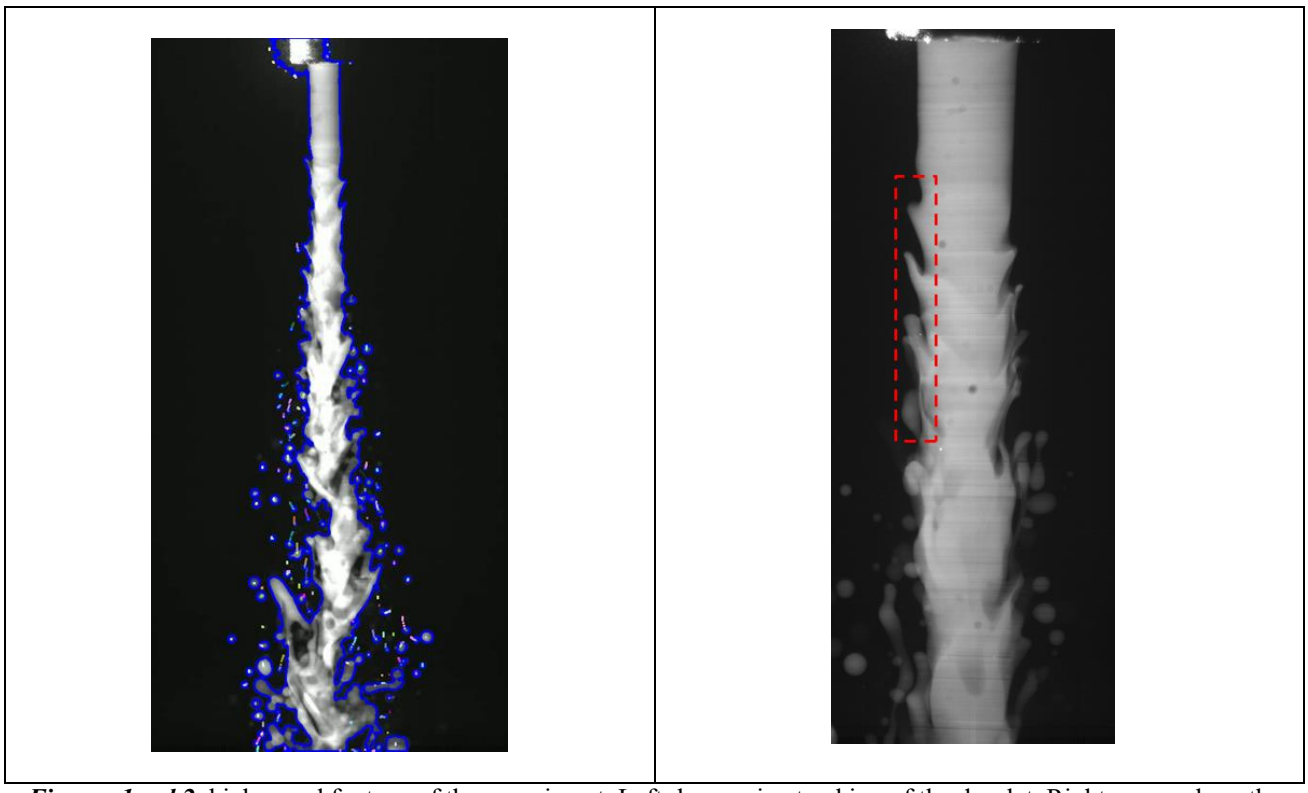

Figures 1and 2: high speed footage of the experiment. Left: lagrangian tracking of the droplet. Right: zone where the DMD analysis is located

References

[1] Schmid, P. (2010). *Dynamic mode decomposition of numerical and experimental data*. Journal of Fluid Mechanics, **656**, 5-28.
[2] Entov, V. M., & Yarin, A. L. (1984). *The dynamics of thin liquid jets in air*. Journal of Fluid Mechanics, **140**, 91-111.
[3] Sterling, A. M., & Sleicher, C. A. (1975). *The instability of capillary jets.* Journal of Fluid Mechanics, **68**(3), 477-495.
[4] Lin, S. P., & Reitz, R. D. (1998). *Drop and spray formation from a liquid jet*. Annual review of fluid mechanics, **30**(1), 85-105.

Entrainment, diffusion and effective compressibility in a self-similar free shear turbulent jet

T. Basset, B. Viggiano, T. Barois, M. Gibert, N. Mordant, R. B. Cal, R. Volk and M. Bourgoin

By considering a turbulent jet inhomogeneously seeded with tracer particles solely injected through the nozzle, we investigate the role of entrainment on the global axial and radial velocity profiles. Our experiment runs in an incompressible self-similar free shear water jet, where we perform Particle Tracking Velocimetry. The jet is seeded with tracers only through the nozzle: inhomogeneous seeding called nozzle seeding. The Lagrangian flow tagged by the tracers therefore does not contain any direct contribution from particles entrained into the jet from the surrounding irrotational fluid. Our measurements reveal that while the mean velocity field extracted from nozzle-seeded tracer trajectories $\langle U_\varphi \rangle$ is essentially indistinguishable from the mean velocity field of the global jet $\langle U \rangle$ for the axial component of velocity, important differences are found for the radial component. We formulate a quantitative explanation for this distinction, by noting that although the global jet is incompressible (the velocity field $\langle U \rangle$ is divergence free, $\nabla \cdot \langle U \rangle = 0$), the nozzle-seeded part if the flow $\langle U_\varphi \rangle$ is effectively compressible ($\nabla \cdot \langle U_\varphi \rangle \neq 0$) as a consequence of mass conservation which, considering the inhomogeneous seeding and the associated non-uniform concentration field $\langle \varphi \rangle$ of nozzle-seeded tracers, imposes that $\nabla \cdot (\langle \varphi \rangle \langle U_\varphi \rangle) = 0$. This allows us to derive new analytical expressions for the contributions of nozzle and entrained particles to the global self-similar profiles of free shear jets, connected to the effective compressibility of the nozzle seeded flow $\langle U_\varphi \rangle$. Finally, we revisit the classical advection-diffusion description of turbulent jets at the light of these novel effective compressibility considerations to derive new analytical expressions for the transport coefficients (eddy diffusivity, eddy viscosity and turbulent Prandtl number) of the turbulent jet, only requiring the knowledge of mean profiles to be accurately estimated, also accounting for their spatial variability.

Optimization of image processing for temperature measurements using Thermochromic Liquid Crystals

B. Turkyilmaz[1], B. Ranjbaran[1], J.O. Rodríguez-García[1], and A. Gylfason[1]
[1] Department of Engineering, Reykjavik University,
Menntavegur 1, 102 Reykjavík, Iceland.

The flow of a fluid heated from below and cooled from above, ultimately resulting in turbulent thermal convection, is widely studied experimentally and numerically. Although turbulent thermal convection has been investigated vastly, a number of issues remain to be fully understood, especially when considering the Lagrangian description of the transport properties of convective turbulence. Temperature, velocity, and acceleration measurements have significance to the investigation of convective flow systems. Nonintrusive measurements of temperature, velocity, and acceleration for convective flows are possible by utilizing color signals of thermochromic liquid crystals (TLCs) and particle image velocimetry (PIV), simultaneously. Our interest lies in advancing Lagrangian detection by combining temperature field measurements based on TLCs and Lagrangian Particle Tracking (LPT).

Temperature field measurements based on TLCs are highly sensitive to image processing as is a relatively new temperature measurement methodology. We intend to advance the methodology used in analyzing TLC calibration and image processing, to meet the requirement of the overall detection system that combines temperature measurements and LPT. The main optimization efforts have centered on color value-temperature calibration process. There appears to be a need to quantify the uncertainty of TLC temperature measurements in the perspective of interrogation window size analogous to PIV which clarifies the relation between interrogation window size and uncertainty of measurement. The directional uncertainties are mostly sourced by optical reasons, such as camera angle and inhomogeneity in illumination. We attempt to eliminate these uncertainties by advancing the image processing procedure. The detailed results and parametric study will be provided in the poster presentation.

Spatial and Temporal Scales of Free-Surface Turbulence

Filippo Coletti
Department of Mechanical and Process Engineering, ETH Zurich

Compared to single-phase three-dimensional turbulence, the transport along the free surface of a turbulent liquid have received limited attention. Past studies in this area have mostly focused on the influence exerted by the surface on the flow underneath, while our understanding of the dynamics along the interface itself remains incomplete.

Here we study the motion of tracer particles floating on the free surface of turbulent water. Experiments are carried out in a large open channel flow facility, over the 1-meter wide and 6-meter long fully developed turbulent region behind a square mesh grid (Figure 1a). Millions of trajectories are reconstructed by particle tracking velocimetry, allowing us to explore single-point and two-point statistics in both the Eulerian and the Lagrangian frames. We focus on a regime in which deformation of the free surface by turbulence is negligible. Despite the tracers being confined to a 2D fluid surface, their motion is consistent with the canonical theory of Kolmogorov for 3D homogeneous isotropic turbulence. This is revealed by the analysis of: the distributions of velocity fluctuations and accelerations; the correlation length scales of the flow; the Eulerian velocity structure functions; the Lagrangian single-particle dispersion; and the particle-pair dispersion. The key turbulence characteristics, including the turbulence dissipation rate and integral length scale of the free surface flow, are consistent with those measured in the bulk by particle image velocimetry. Still, the peculiar aspects of the free-surface transport are evident from the effective compressibility of the velocity field: the floating tracers display intense clustering, as quantified by radial distribution functions and Voronoi diagram analysis. The clusters extend over spatial and temporal scales comparable to the integral scales of the turbulence.

When the floaters' concentration is increased up to covering a significant fraction (up to ~20%) of the free surface, the inter-particle interactions profoundly alter the transport: the particles aggregate and stick to each other due to capillary effects, forming large fractal clusters that move as a whole (Figure 1b). Furthermore, analysis of the Lagrangian dispersion and relative velocities of the dense floaters reveal the effect of the increasing concentration on the spreading rate, in comparison to the dilute case.

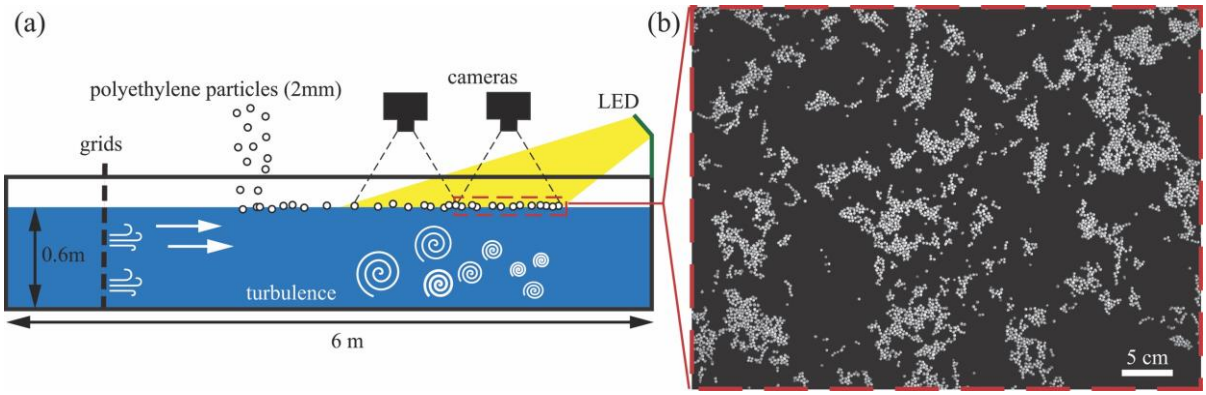

Figure 1: (a) Schematics of the experimental setup. (b) Typical snapshot of particle clusters floating on the free surface of the turbulent water flow.

High-order statistics and intermittency of a two-fluid HVBK quantum turbulent flow

Zhentong Zhang,[1,*] Ionut Danaila,[1,†] Emmanuel Lévêque,[2,‡] and Luminita Danaila[3,§]

[1] *Université de Rouen Normandie, Laboratoire de Mathématiques Raphaël Salem, CNRS UMR 6085, Avenue de l'Université, 76801 Saint-Étienne-du-Rouvray, France*

[2] *Laboratoire de Mécanique des Fluides et dAcoustique, École Centrale de Lyon, CNRS UMR 5509, 36, avenue Guy de Collongue, Lyon, France*

[3] *Université de Rouen Normandie, Laboratoire Morphodynamique continentale et côtière, CNRS UMR 6143, Place Emile Blondel, 76821 Mont Saint Aignan, France*

(Dated: April 3, 2022)

The Hall-Vinen-Bekharevich-Khalatnikov (HVBK) model is widely used to numerically study quantum turbulence in superfluid helium. Based on the two-fluid model of Tisza and Landau, the HVBK model describes the normal (viscous) and superfluid (inviscid) components of the flow using two Navier-Stokes type equations, coupled through a mutual friction force term. This feature makes the HVBK model very appealing in applying statistical tools used in classical turbulence to study properties of quantum turbulence. A large body of literature used low-order statistics (spectra, or second-order structure functions in real space) to unravel exchanges between the two fluids at several levels. The novelty in this study is to use a theoretical approach based on first principles to derive transport equations for the third-order moments for each component of velocity. New equations involve the fourth-order moments, which are classical probes for internal intermittency at any scale, revealing the probability of rare and strong fluctuations. Budget equations are assessed through Direct Numerical Simulations (DNS) of the HVBK flow based on accurate pseudo-spectral methods. We simulate a forced homogeneous isotropic turbulent flow with Reynolds number of the normal fluid (based on Taylor's microscale) close to 100. Values from 0.1 to 10 are considered for the ratio between the normal and superfluid densities. For these flows, an inertial range is not discernible and the Restricted Scaling Range (RSR) approach is used to take into account the Finite Reynolds Number (FRN) effect. We analyse the importance of each term in budget equations and emphasize their role in energy exchange between normal and superfluid components. Some interesting features are observed: i) transport and pressure-related terms are dominant, similarly to single-fluid turbulence; ii) the mathematical signature of the FRN effect is weak in the transport of the third-order moment, despite the low value of the Reynolds number; iii) for very low temperatures, the normal fluid behaves in the RSR as a fluid of vanishing viscosity, since the mutual friction annihilates the effects of viscosity. We also derive the equation for the velocity flatness F for small scales. We show that F of the normal fluid gradually increases when temperature decreases. The flatness of the superfluid first increases, and then falls for low temperatures. This result corroborate the picture of the temperature-depending dynamics of the superfluid component.

* Email: zhentong.zhang@univ-rouen.fr
† Email: ionut.danaila@univ-rouen.fr
‡ Email: emmanuel.leveque@ec-lyon.fr
§ Email: luminita.danaila@univ-rouen.fr, Corresponding author

Modulation of homogeneous and isotropic turbulence in emulsions

Sergio Chibbaro, Marco Crialese Esposito, Luca Brandt

Université Paris-Saclay, CNRS LISN 91400 Orsay France

FLOW Centre, KTH Royal Institute of Technology, Stockholm, Sweden

We present a numerical study of emulsions in homogeneous and isotropic turbulence at Taylor Re=137. The problem is addressed via Direct Numerical Simulations (DNS), where the Volume of Fluid (VOF) is used to represent the complex features of the liquid-liquid interface. We consider a mixture of two iso-density fluids, where fluid properties are varied with the goal of understanding their role in turbulence modulation, in particular the volume fraction, viscosity ratio and large scale Weber number. The analysis, performed by studying integral quantities and spectral scale-by-scale analysis, reveals that energy is consistently transported from large to small scales by the interface, and no inverse cascade is observed. Furthermore, the total surface is found to be directly proportional to the amount of energy transported, while viscosity and surface tension alter the dynamic that regulates energy transport. We also observe the 10/3 and 3/2 scaling on droplet size distributions, suggesting that the dimensional arguments which led to their derivation are verified in HIT conditions.

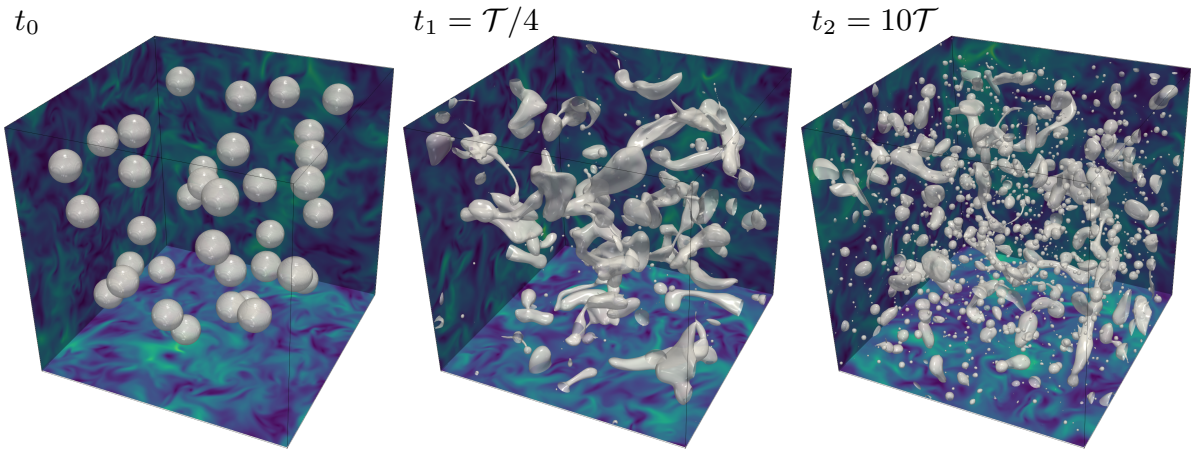

Fascinating interface topology and dynamics in micro mixers

M.V. Salvetti, A. Mariotti, M. Antognoli, S. Tomasi Masoni, E. Brunazzi, C. Galletti, R. Mauri
Dipartimento di Ingegneria Civile e Industriale, Università di Pisa (Italy)

Microfluidic devices have several interesting features and are receiving much attention for the intensification of many processes in the fine chemical, pharmaceutical, and food industries.
The challenge is to obtain efficient mixing between the flow streams entering the mixer at low Reynolds numbers, Re, due to the small dimensions of the devices, and for simple geometries, which may be easily integrated in device networks. This happens if the flow symmetries are broken, and mixing is promoted by splitting and recombination of the interface between the flow streams. We consider here two widely studied mixer geometries, i.e., T and X configurations, fed by different fluids which may eventually react. Numerical simulations, experimental flow visualizations, and PIV are used jointly to investigate the flow features and mixing in these configurations. Despite the simple geometry and laminar flow conditions, they exhibit a rich and very complex fluid mechanical behavior, depending on Re. At low Reynolds number, the two streams remain stratified in the mixing channels due to their different densities, and mixing is promoted only by diffusion. By increasing the Reynolds number, the engulfment regime occurs, which is characterized by the presence of vortical structures (different in T- and X-microreactors) in the confluence region and in the outlet channels, which lead to the distortion of the interface between the fluids and promote mixing thanks to convection. Upon further increasing Re, the fluid flow becomes unsteady and time periodic. Figure 1 shows, for instance, the experimental flow visualizations and the vortical structures obtained numerically at different time instants for a T-mixer at Re=320. A blob of vorticity is shed from the confluence region into the outlet channel. The interface between the two fluid streams, which is clearly visualized by the streaks in the experimental flow images, is distorted by the passage of the vorticity blob. This consequently gives a boost to the mixing between the two streams.
In this presentation, the unsteady flow regimes in T and X micro-mixer will be described together with the related dynamics of the interface between the flow streams. The implications on mixing will be discussed. The unsteady periodic flow regimes are the step before the turbulent chaotic dynamics occurring at slightly larger Re.

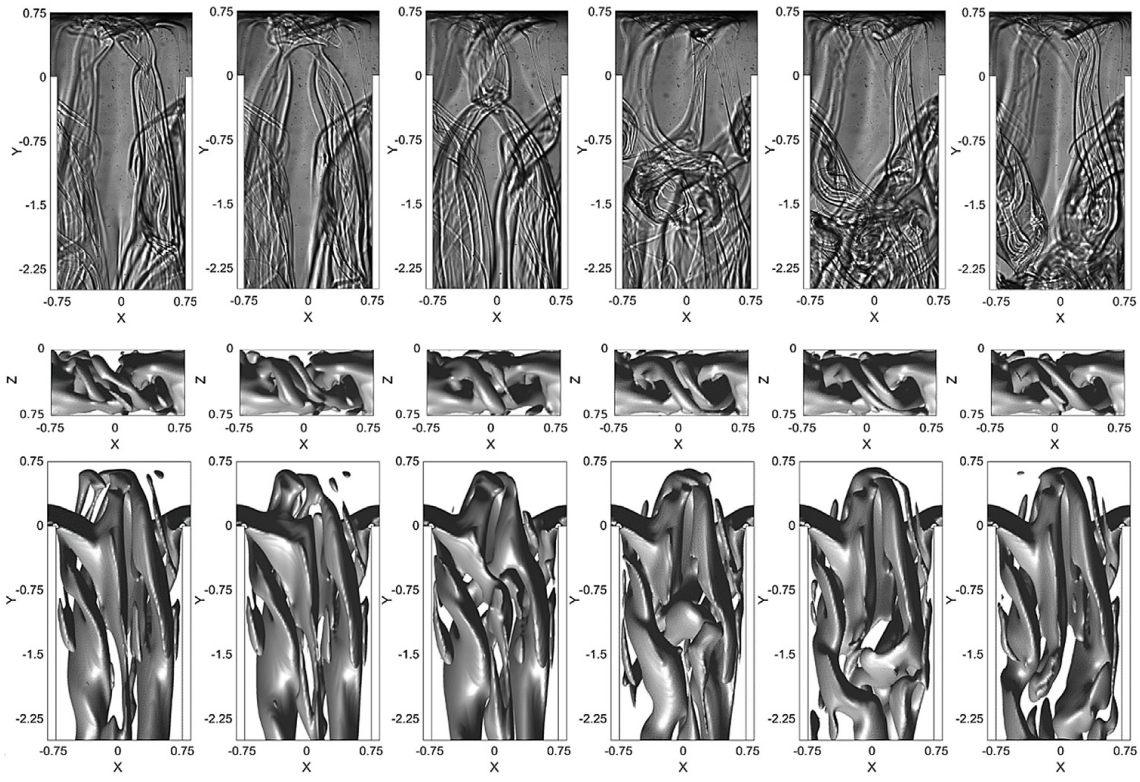

Figure 1: experimental flow visualizations and vortical structures obtained numerically at different time instants for a T-mixer at Re=320.

Drag reduction in turbulent pipe flows of realistic polymer solutions

F. Serafini[1], F. Battista[1], P. Gualtieri[1] and C.M. Casciola[1]
[1] Department of Mechanical and Aerospace Engineering,
Sapienza University of Rome, via Eudossiana 18, 00184 Roma.

Tom's effect, namely the drag-reducing capability of polymers in turbulence, is debated since its discovery in the 40s, see Virk (1975). Viscoelastic models (e.g FENE-P, finitely extensible nonlinear elastic model with Peterlin's approximation) achieve drag reduction in numerical simulations of prototypal flows. These models require unrealistically large concentrations to obtain drag reduction, well beyond the model limit of validity. Furthermore, many laboratory-scale experiments are performed at Weissenberg numbers unreachable by the viscoelastic models. Direct Numerical Simulations data of DNA macromolecules, modeled as FENE dumbbells, fully coupled to the Newtonian fluid are discussed. A hybrid Eulerian-Lagrangian approach is used to evolve every single dumbbell. The Exact Regularized Point Particle method is used to exactly account for the momentum coupling between the two phases, see Gualtieri et al. (2015) for details. The left panel of the figure shows an instantaneous cross-section of axial vorticity, ζ_z, and polymer configuration at $Wi = 10600$. The right panel shows the mean axial velocity profiles as a function of the radial coordinate for different values of the Weissenberg number. The drag reduction is shown to increase with the Weissenberg number. Methodological details and a physical explanation of the drag reduction mechanism will be provided in the oral presentation.

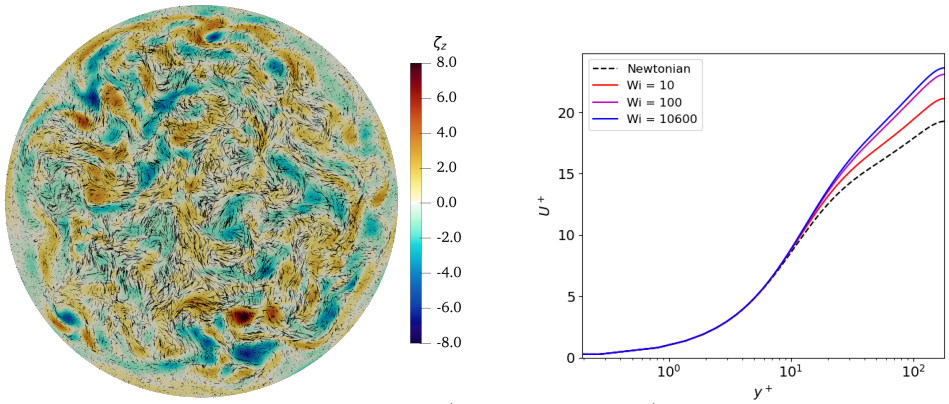

Figure 1: Instantaneous axial vorticity (colored contour), instantaneous polymer configuration (black lines) on a pipe cross-section: left panel. Mean velocity profiles at increasing Weissenberg numbers: right panel.

References

Paolo Gualtieri, F Picano, Gaetano Sardina, and Carlo Massimo Casciola. Exact regularized point particle method for multiphase flows in the two-way coupling regime. *Journal of Fluid Mechanics*, 773:520–561, 2015.

Preetinder S Virk. Drag reduction fundamentals. *AIChE Journal*, 21(4):625–656, 1975.

On the modelling and simulation of the dynamic of charged particles in turbulent flow

A. Boutsikakis, P. Fede, O. Simonin
Institut de Mécanique des Fluides de Toulouse (IMFT)
Université de Toulouse, CNRS

Turbulent particle-laden flows are encountered in many practical applications such as geophysical flows, engineering processes or health/medicine studies. The modelling and simulation of particle transport and dispersion is complex due to the multi-physical nature of particle-laden flows. A non-exhaustive list includes particle-turbulence interaction, inter-particle collisions or particle bouncing on a smooth or rough wall. In addition, although long neglected in modelling approaches, the effect of electric charges on the dynamics of particle flow can be very important. The objective of this talk is to present some recent advances in modelling and simulation of transport and dispersion of electrically charged particles in turbulent flows.

The presentation is focusing on the effect of electrostatic forces on the dynamic of small inertial particles, with the same charge, transported by a homogeneous isotropic turbulent flow, for very dilute configurations. This phenomenon is analyzed from direct numerical simulation (DNS) of gas turbulent flows coupled with Lagrangian tracking of discrete solid particles (figure 1). The simulation results show that the self-dispersion and segregation of the particles decrease with increasing electric charge. In contrast, the kinetic energy of the particles can increase or decrease with respect to the electric charge (figure 2) depending on the inertia of the particle. Statistical analysis of the simulation results, in the frame of the fluid-particle joint PDF approach, shows that the change in the kinetic energy of the charged particles is only due to a change in the efficiency of entrainment by the fluid turbulence characterized by the fluid-particle velocity covariance. Secondly, the prediction of the covariance with electrostatic effects is the result of a competition between a change in the correlation between fluid acceleration and particle velocity and a direct decorrelation effect between fluid and particle velocities by the electrostatic forces acting on the particles. Such a decorrelation effect can be modelled by introducing a Coulomb collision cross section by analogy with the elastic collision effect on particle dispersion in turbulent flows.

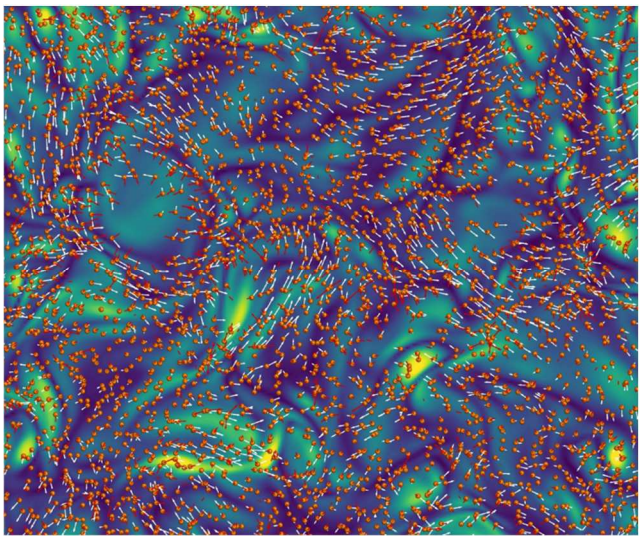

Figure 1: Fluid turbulent vorticity field and instantaneous distributions of electrostatic forces and particle velocities in homogeneous isotropic forced turbulence.

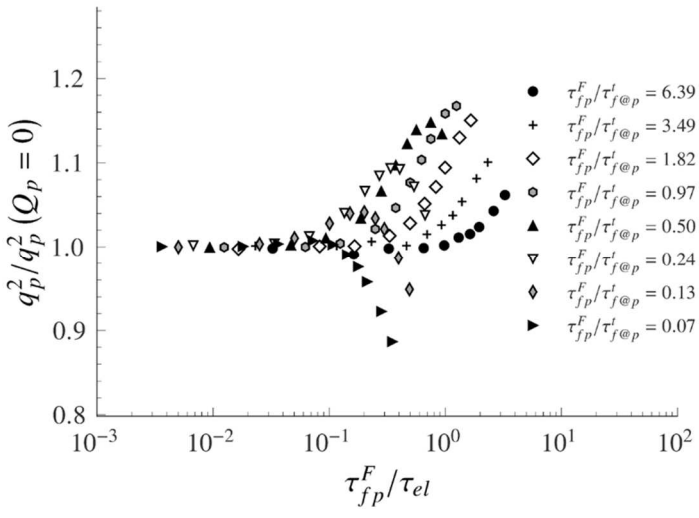

Figure 2: Kinetic energy of charged particles in homogeneous isotropic forced turbulence as a function of an electrostatic Stokes number.

BOUTSIKAKIS, A., FEDE, P., PEDRONO, A., SIMONIN, O., 2020, "Numerical simulations of short- and long-range interactions forces in turbulent particle-laden gas flows", *FLOW TURBULENCE COMBUST.*, VOL. 105, PP. 989-1015.

BOUTSIKAKIS, A., FEDE, P., SIMONIN, O., 2022, " Effect of electrostatic forces on the dispersion of like-charged solid particles transported by homogeneous isotropic turbulence", *J. Fluid Mech.*, Vol. 938, A33.

Inertial deformable particles in turbulence

B. Favier, P. Le Gal and G. Verhille
Institut de Recherche sur les Phénomènes Hors Equilibre (IRPHE)
Aix-Marseille Univ, Centrale Marseille, CNRS

Most of the studies on deformable particles in turbulent flows deal either with bubbles [1] or polymers [2] and have mainly been motivated by drag reduction. However, in several fields, flexible objects are transported by turbulent flows. For instance, plastic litters such as plastic bags, fishing lines, ... are advected by oceanic current and can be distorted and even fragmented by turbulent fluctuations occurring during storms [3]. Another example in industrial flows is the manufacturing of paper where pulp fibers which can be flexible, are advected, oriented and aggregated by flows [4]. In these different examples, the particles are generally larger than the Kolmogorov length and Brownian fluctuations are negligible. Therefore deformations are solely due to the turbulent fluctuations. Recently our team and few others have started to investigate this regime of deformation and their influence on the particle dynamics. Here, I will firstly characterize the transition from rigid to flexible regime for both fibers (1D particle) and discs (2D particle). I will then discuss the statistics of the deformation and one direct application to the modelling of the formation of microplastic in the ocean.

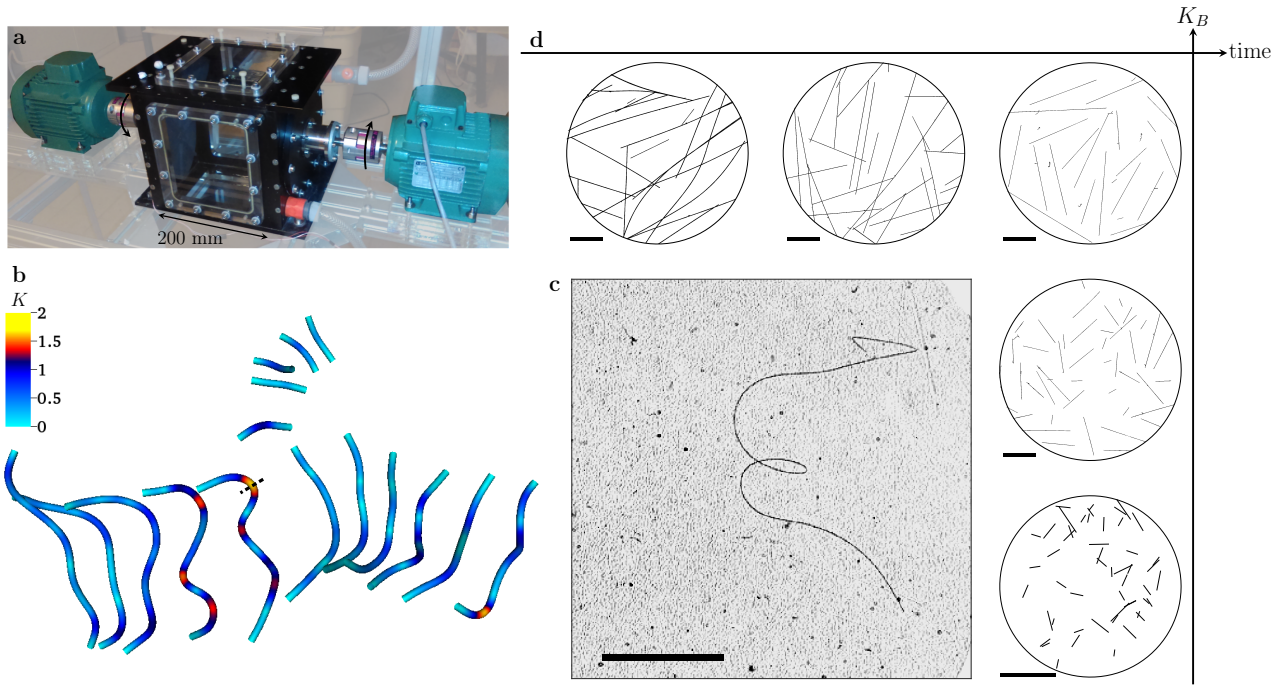

Fragmentation of brittle fibers in turbulent flows. a) Picture of the von Kármán flow used to study fiber fragmentation. b) Breakup event obtained in the numerical simulations. c) 2D image of a glass fiber deformed by the experimental turbulent flow observed using a schlieren technique. d) Random sets of fiber fragments collected in the experimental turbulent flow, for different times and breaking parameters KB. The scale bars in panels (c) and (e) all indicate 10 mm. [3]

Bibliography:

[1] D. Lohse, Bubble puzzles: From fundamentals to applications, *Phys. Rev. Fluids*, 3(11), 110504, 2018.
[2] R. Benzi and E.S.C Ching, Polymers in fluid flows, *Annu. Rev. Cond. Matt. Phys.*, 9, 163-181, 2018.
[3] C. Brouzet *et al.*, Laboratory model for plastic fragmentation in the turbulent ocean, *Phys. Rev. Fluids*, 6, 024601, 2021.
[4] F. Lundell *et al.*, Fluid mechanics of papermaking, *Annu. Rev. Fluid Mech.*, 43, 195-217, 2011.

Influence of density and viscosity on deformation, breakage and coalescence of bubbles in turbulence

A. Soldati[1,2], F. Mangani[1] and A. Roccon [1,2]
[1] Institute of Fluid Mechanics and Heat Transfer, TU Wien, Vienna 1060, Austria
[2] Polytechnic Department, University of Udine, 33100 Udine, Italy

We numerically investigate the effect of density and viscosity differences on a swarm of large and deformable bubbles dispersed in a turbulent channel flow. For a given shear Reynolds number, $Re_\tau = 300$, and a constant bubble volume fraction, $\Phi = 5.4\%$, we perform a campaign of direct numerical simulations (DNS) of turbulence coupled with a phase-field method (PFM) accounting for interfacial phenomena. For each simulation, we vary the Weber number (We, ratio of inertial to surface tension forces), the density ratio (ρ_r, ratio of bubble density to carrier flow density) and the viscosity ratio (η_r, ratio of bubble viscosity to carrier flow viscosity). Specifically, we consider two Weber numbers, $We = 1.50$ and $We = 3.00$, four density ratios, from $\rho_r = 1$ down to $\rho_r = 0.001$ and five viscosity ratios from $\eta_r = 0.01$ up to $\rho_r = 100$. Our results show that density differences have a negligible effect on breakage and coalescence phenomena, while a much stronger effect is observed when changing the viscosity of the two phases. Increasing the bubble viscosity with respect to the carrier fluid viscosity damps turbulence fluctuations, makes the bubble more rigid and strongly prevents large deformations, thus reducing the number of breakage events. Local deformations of the interface, on the contrary, depend on both density and viscosity ratios: as the bubble density is increased, a larger number of small-scale deformations, small dimples and bumps, appear on the interface of the bubble. The opposite effect is observed for increasing bubble viscosities: the interface of the bubbles become smoother. We report that these effects are mostly visible for larger Weber numbers, where surface forces are weaker. Finally, we characterize the flow inside the bubbles:As the bubble density is increased, we observe an increase in the vorticity inside the bubble, while as the bubble viscosity is increased, we observe a mild reduction of the vorticity inside the bubble and a strong suppression of turbulence [1]. A similar result can be observed in terms of turbulent kinetic energy (TKE), a decrease of the density ratio or an increase of the viscosity ratio implies a lower Reynolds number inside the bubbles and turbulent structures are suppressed, while an increase of the density ratio or a decrease of the viscosity ratio produces a higher Reynolds number and thus finer turbulent structures.

[1] Mangani et al. *Phys. Rev. Fluids* 2022, Submitted)

Dynamics of bubble-induced turbulence from coarse-grained simulations

F. Le Roy de Bonneville[1,2], R. Zamansky[1], F. Risso[1], A. Boulin[2], J.-F. Haquet[2]
[1]*Institut de Mécanique des Fluides de Toulouse (IMFT), CNRS, Université de Toulouse, France*
[2]*SMTA, LMAG, CEA, DEN, DTN, 13108 Saint-Paul-Lez-Durance, France*

We report numerical simulations of a homogeneous swarm of bubbles rising at large Reynolds number, $Re = 760$, corresponding to air bubbles of diameter d=2.5 mm rising in water, at a gas volume fraction α from 1 to 7.5%. The liquid phase is described by solving, on an Eulerian grid, the Navier-Stokes equations, including sources of momentum which model the effect of the bubbles. The dynamics of each bubble is determined in a Lagrangian framework by solving an equation of motion involving the hydrodynamic forces exerted by the fluid. The computation of the drag and added-mass forces requires to remove the velocity disturbance generated by a bubble in the vicinity of itself from the total computed velocity field. An original method has been developed for this purpose and validated by comparison with experiments [1]. It allows us to perform coarse-grained simulations (Fig. 1a) with less than 15 mesh-grid spacings per bubble diameter, which proved to reliably describe the dynamics of the resolved flow scales.
These simulations have been processed to analyze the dynamics of the bubble-induced liquid fluctuations. First, the average liquid disturbance generated around each bubble has been determined by means of conditional averaging. This allows us to discriminate the contribution to the liquid velocity fluctuations of the *Localized Bubble Disturbances* (LBD) from that of the real *Bubble-Induced Turbulence* (BIT) [2]. Then, spectral budgets of the energy of the LBD and BIT have been computed, shedding light on the mechanisms of the turbulence. The work of the buoyancy supplies energy to the LBD on a range of wavelengths of less than one decade, located just above the bubble scale. A small part of this energy is directly dissipated into heat while the major part is converted into turbulence. The BIT budget is shown in Fig. 1b. The production of turbulence by the LBD (P) is distributed around a peak that is located at a smaller wavenumber than the peak of the dissipation (D). However, at variance with high-Reynolds number single-phase flow turbulence, there is no clear scale separation between P and D, resulting in a significant transfer term (T). Note that the well-known k^{-3} regime of the energy spectrum, signature of the BIT, starts beyond the maximum of D, where P and D are decreasing functions of k. It thus implies a subtle balance between production, transfer and dissipation.

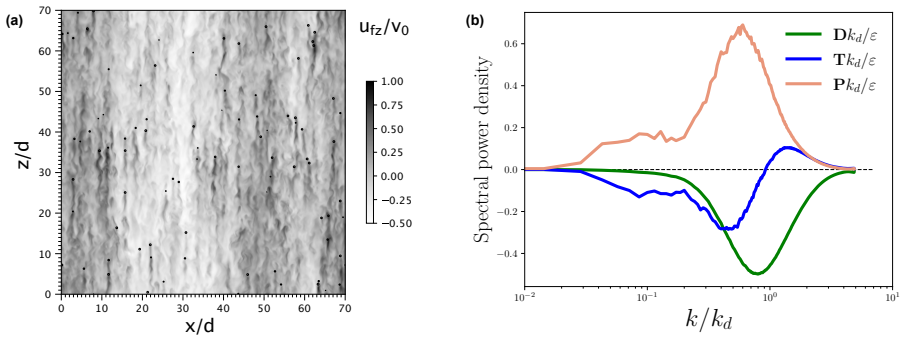

Figure 1: Numerical results at $\alpha = 2\%$. (a) Snapshot of the vertical liquid velocity. (b) Spectral budget of the turbulence induced by the bubbles (BIT). The spectral densities of production (P), transfer (T) and dissipation (D) are normalized by the bubble wavenumber k_d and the dissipation rate ϵ , and plotted versus k/k_d.

References

[1] F. Le Roy De Bonneville, R. Zamansky, F. Risso, A. Boulin, & J.-F. Haquet, *Numerical simulations of the agitation generated by coarse-grained bubbles moving at large Reynolds number.* J. Fluid Mech. **926**, A20 (2021)

[2] F. Risso, *Agitation, mixing, and transfers induced by bubbles.* Ann. Rev. Fluid Mech. **50**, 25-48 (2018)

Multiscale techniques for analyzing voids and clusters in particle-laden turbulence

Kai Schneider
I2M - UMR 7373/CNRS, Centre de Mathematiques et d'Informatique, Aix-Marseille Universite

Abstract:

Multiscale statistical analyses of inertial particle distributions are presented to investigate the statistical signature of clustering and void regions in particle-laden incompressible isotropic turbulence. Three-dimensional direct numerical simulations of homogeneous isotropic turbulence at high Reynolds number ($Re_\lambda \gtrsim 200$) with up to 10^9 inertial particles are performed for Stokes numbers ranging from 0.05 to 5.0.

A finite-time measure to quantify divergence and the rotation of the particle velocity by determining respectively the volume change rate of the Voronoi cells and their rotation is proposed. For inertial particles the probability distribution functions (PDF) of the divergence and of the curl deviate from that for fluid particles. Joint PDFs of the divergence and the Voronoi volume illustrate that the divergence is most prominent in cluster regions and less pronounced in void regions. For larger volumes the results show negative divergence values which represent cluster formation and for small volumes the results show positive divergence values which represents cluster destruction/void formation. Moreover, when the Stokes number increases the divergence takes larger values, which gives some evidence why fine clusters are less observed for large Stokes numbers. Finally, the PDFs of the particle vorticity have much heavier tails compared to the fluid vorticity, and the extreme values increase significantly with the Stokes number.

Orthogonal wavelet analysis is then applied to the computed particle number density fields. Scale-dependent skewness and flatness values of the particle number density distributions are calculated and the influence of Reynolds number Re_λ and Stokes number St is assessed. For $St \sim 1.0$, both the scale-dependent skewness and flatness values become larger as the scale decreases, suggesting intermittent clustering at small scales. For $St \leq 0.2$, the flatness at intermediate scales, i.e. for scales larger than the Kolmogorov scale and smaller than the integral scale of the flow, increases as St increases, and the skewness exhibits negative values at the intermediate scales. The negative values of the skewness are attributed to void regions. These results indicate that void regions at the intermediate sales are pronounced and intermittently distributed for such small Stokes numbers.

This is joint work with Thibault Oujia (Aix-Marseille U, France), Keigo Matsuda (JAMSTEC, Japan) and Katsunori Yoshimatsu (Nagoya U, Japan).

Ref.:

T. Oujia, K. Matsuda and K. Schneider. Divergence and convergence of inertial particles in high Reynolds number turbulence. J. Fluid Mech., 905, A14, 2020.

K. Matsuda, K. Schneider and K. Yoshimatsu. Scale-dependent statistics of inertial particle distribution in high Reynolds number turbulence. Phys. Rev. Fluids, 6, 064304, 2021.

S. V. Apte, T. Oujia, K. Matsuda, B. Kadoch, X. He and K. Schneider. Clustering of inertial particles in turbulent flow through a porous unit cell. J. Fluid Mech., 937, A9, 2022.

Broken mirror symmetry of tracer's trajectories in turbulence

Sofía Angriman[1], Pablo Cobelli[1], Mickaël Bourgoin[2], **Sander Huisman[3]**, Romain Volk[2], Pablo Mininni[1]

[1]Universidad de Buenos Aires, Facultad de Ciencias Exactas y Naturales, Departamento de Fisica, & IFIBA, CONICET, Ciudad Universitaria, Buenos Aires 1428, Argentina

[2]Université Lyon, ENS de Lyon, Université Claude Bernard, CNRS, Laboratoire de Physique, 46 Alleé d'Italie F-69342 Lyon, France

[3]Physics of Fluids Group, Max Planck UT Center for Complex Fluid Dynamics, Faculty of Science and Technology, MESA+ Institute and J.M. Burgers Centre for Fluid Dynamics, University of Twente, P.O. Box 217, 7500 AE Enschede, Netherlands

---

Topological properties of physical systems play a crucial role in our understanding of nature, yet their experimental determination remains incredibly hard or nearly impossible. We show that the helicity, a dynamical invariant in ideal flows, quantitatively affects trajectories of fluid elements: the mean (modified) linking number of Lagrangian trajectories depends on the helicity. Thus, a global topological invariant and a topological number of fluid trajectories become related, and we provide an empirical expression linking them. We show various types of experimental and numerical data from three fluid-dynamical geometries: von Kármán, HIT flow, and Taylor-Green turbulence confirming this relation. Furthermore, from this relation we can show the existence of long-term memory in the trajectories: the links can be made of the trajectory up to a given time, with particles positions in the past. This property provides us a relatively easy way to experimentally measure the helicity.

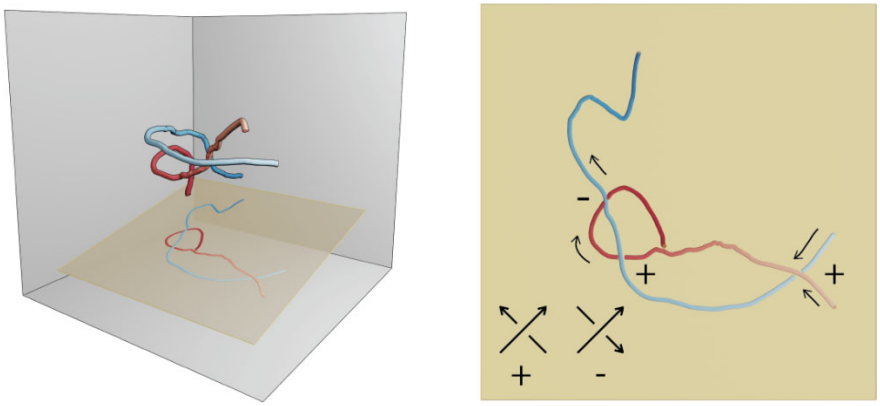

Figure 1: Trajectory of two particles in 3D, and their 2D projection on to the plane shown. Their 2D crossings are signed accordingen to the direction of the trajectories.

Herman Clercx, Matteo Madonia, Andrés Aguirre Guzmán,
Xander de Wit and Rudie Kunnen
Fluids and Flows group, Department of Applied Physics,
Eindhoven University of Technology, Eindhoven, The Netherlands

Turbulent rotating Rayleigh-Bénard convection: Flow organization and heat transfer in slender confined cylinders

Most geo- and astrophysical flows are driven by strong thermal forcing and affected by high rotation rates. In these systems, direct measurements of the physical quantities are not possible due to their large scales, remoteness and complexity. Turbulent rotating Rayleigh-Bénard convection (RRBC) represents a model that contains the main physical constituents: it consists of a rotating fluid layer heated from below and cooled from above. Two approaches are generally popular to investigate flow and transport properties of RRBC under these extreme conditions: 1) laboratory experiments in (slender) cylindrical convection cells and 2) numerical simulations of thermally-driven turbulence in horizontally-periodic domains between parallel (heated and cooled) plates.

Background rotation causes different flow structures and heat transfer efficiencies in turbulent RRBC. Three main regimes are known: rotation-unaffected (regime I), rotation-affected (regime II) and rotation-dominated (regime III). Regimes I and II are easily accessible with experiments and numerical simulations, thus they have been extensively studied during the last two decades, see for a recent review [1]. On the other hand, access to regime III is more challenging [2,3]. We will focus in this talk on regime III, including the geostrophic turbulence regime. With the experimental setup TROCONVEX [4], through its huge dimensions (up to 4 m tall), an investigation of parameters closer than ever before to the ones of geo- and astrophysical flows has become possible. Results from flow measurements based on this unique experimental setup, using stereoscopic particle image velocimetry in a horizontal plane at mid-height, will be presented. We will in particular discuss the remarkable quadrupolar organization of the flow in that plane [3]. This is in strong contrast with the well-known large-scale vortex observed in many numerical studies of RRBC on horizontally-periodic domains. A significant discrepancy in total heat transport is observed between experimental data obtained from the confined cylindrical domain (like TROCONVEX) and numerical data obtained from simulations on a horizontally-periodic domain. This discrepancy is further explored with direct numerical simulations on a cylindrical domain [5]. An analysis of the flow field reveals a region of enhanced convection near the wall, the sidewall circulation. It is this sidewall circulation that accounts for the differences in heat transfer between these two canonical systems (cylindrical versus periodic domain), while in the bulk the turbulent heat flux is the same for both systems. The latter implies that bulk measurements of heat transfer in cylindrical convection cells are representative for heat transfer in laterally unbounded (or horizontally-periodic) domains, at least for the parameter regime under consideration.

[1] R. Stevens, H. Clercx & D. Lohse, EJMB/F **40**, 41-49 (2013).
[2] H. Rajaei, R. Kunnen & H. Clercx, PoF **29**, 045105 (2017).
[3] M. Madonia, A. Aguirre Guzmán, H. Clercx & R. Kunnen, EPL **135**, 54002 (2021).
[4] R. Kunnen, European Research Council (ERC), grant number 678634.
[5] X. de Wit, A. Aguirre Guzman, M. Madonia, J. Cheng, H. Clercx & R. Kunnen, PRF **5**, 023502 (2020).

Gravitational settling of inertial particles in homogeneous isotropic turbulence

M. Obligado[1], A. Ferran[1,2], N. Machicoane[1], N. Mordant[1] and A. Aliseda[2]
[1] Univ. Grenoble Alpes, CNRS, Grenoble INP, LEGI, 38000 Grenoble, France
[2] Dep. Mechanical Engineering, University of Washington, Seattle, USA

Turbulent flows laden with particles are relevant in environmental phenomena and industrial systems. Despite their relevance is such environments, there remain many open questions concerning the coupling of inertial particles with turbulent flows. In particular, particles immersed in a turbulent flow can see their settling velocity both enhanced or hindered compared to their terminal velocity in a stagnant fluid. The scaling laws and mechanisms responsible for the settling velocity modification have not been yet properly understood.

This study focuses on the gravitational settling of dense sub-Kolmogorov inertial particles in turbulent gas flows. Turbulence is generated in a wind tunnel by means of active and passive grids, in a way that it is close to homogeneous and isotropic for all conditions studied. Experimental measurements of particle vertical and horizontal velocities were taken via a Phase Doppler Interferometer, that can also measure de diameter of particles on the vertical direction. Our experimental setup allowed to explore a wide range of Taylor-scale based Reynolds numbers ($Re_\lambda \in [30-520]$), Rouse numbers ($Ro \in [0-5]$) and volume fractions ($\phi_v \in [0.5\times10-5-2.0\times10-5]$). Three types of grid turbulence were tested by means of a passive grid and an active grid used in two different modes (grid shafts moving randomly or open in a static configuration).

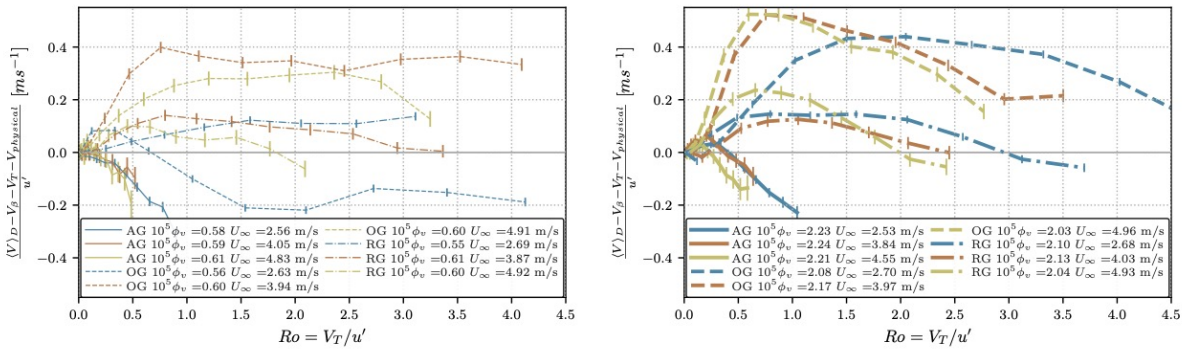

Figure 1: Particle settling velocity normalized with the carrier phase rms velocity plotted against the Rouse number for a volume fraction of 0.5×10^{-5} (left) and 2.0×10^{-5} (right). The data from the active grid in random mode (AG) correspond to solid lines, the one from the active grid in open mode (OG) is in dashed lines and the dashed dotted lines correspond to the data for the passive grid (RG).

This work therefore aims at studying the role of the carrier phase Taylor Reynolds number, Rouse number and volume fraction on the settling velocity of inertial particles (figure 1). We find, in agreement with previous works, that enhancement of the settling velocity occurs at low Rouse number, while hindering of the settling occurs at higher Rouse number for decreasing turbulence energy levels (characterized by the velocity fluctuating

intensity or the Taylor Reynolds number). The wide range of flow parameters explored allowed us to observe that enhancement decreases significantly with the Taylor Reynolds number and is also significantly affected by the volume fraction ϕ_v.

Particle capture by large deformable drops in turbulent flow

Cristian Marchioli[1,2], Arash Hajisharifi[1], Alfredo Soldati[3,1], etc.
[1] *Dept. Engineering and Architecture, University of Udine, 33100 Udine, Italy*
[2] *Dept. Fluid Mechanics, CISM, 33100, Italy*
[3] *Institute of Fluid Mechanics and Heat Transfer, TU Wien, 1060 Wien, Austria*

The capture of neutrally buoyant, sub-Kolmogorov particles at the interface of deformable drops in turbulent flow and the subsequent evolution of particle surface distribution are investigated. Direct numerical simulation of turbulence, phase-field modelling of the drop interface dynamics and Lagrangian particle tracking are used. Particle distribution is obtained considering excluded-volume interactions, i.e. by enforcing particle collisions. Our results, which refer to a turbulent channel flow at shear Reynolds number Re=150 based on the half channel height, show that particles are transported towards the interface by jet-like turbulent motions and, once close enough, are captured by interfacial forces in regions of positive surface velocity divergence. These regions appear to be well correlated with high-enstrophy flow topologies that contribute to enstrophy production via vortex compression or stretching [1].
The rate at which particles get trapped at the interface is observed to scale with the turbulent kinetic energy of the fluid measured within one Kolmogorov length scale from the drop: This scale corresponds to a distance slightly longer than the particle stopping distance, which can be chosen as reference scaling length for the selection of the volume-averaging thickness. This finding can be explained by considering that in our flow configuration, particle capture is driven by the turbulent fluctuations in the vicinity of the drop interface. Once captured by the interfacial forces, particles disperse on the surface. Excluded-volume interactions bring particles into long-term trapping regions where the average surface velocity divergence sampled by the particles is zero. These regions correlate well with portions of the interface characterized by higher-than-mean curvature [2]. This finding is relevant for the understanding of the effect that particles may have on the drop surface properties, in particular surface tension. The convex portions of the interface will be those where changes of the surface tension and, hence, of drop deformability induced by the presence of very small particles will be larger.

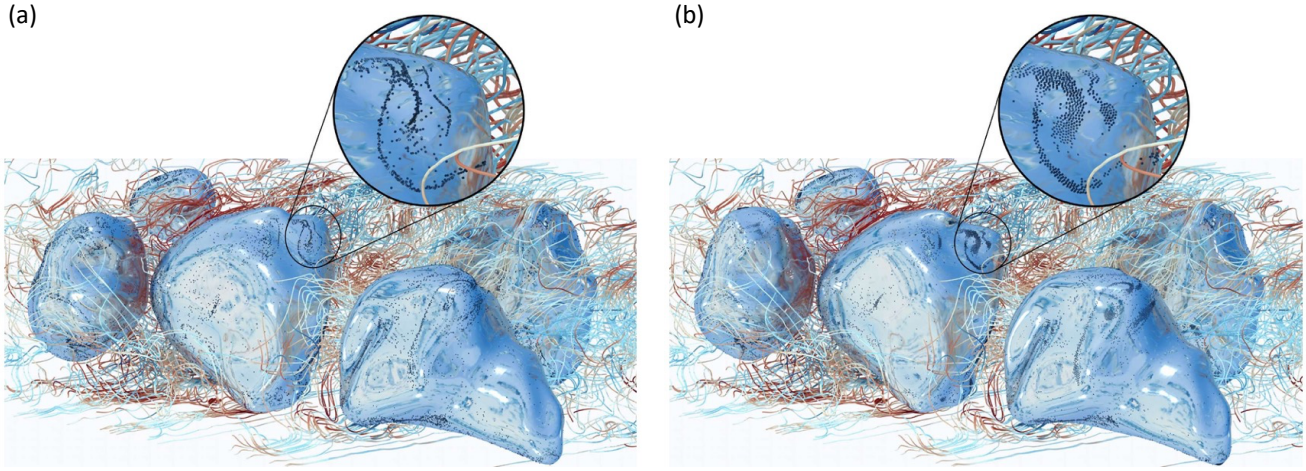

Figure 1: Snapshot of particle distribution on the drop surface. Trapped particles form highly-concentrated filamentary clusters without EVE (panel a), but appear more evenly distributed when EVE are accounted for (panel b). Regions of strong particle accumulation are the same in either case. Picture taken from [2].

References

[1] Hajisharifi A., Marchioli C., and Soldati A., *Particle capture by drops in turbulent flow*. Phys. Rev. Fluids, **6**, 024303 (2021)
[2] Hajisharifi A., Marchioli C., and Soldati A., *Interface topology and evolution of particle patterns on deformable drops in turbulence.* J. Fluid Mech. **933**, A41 (2022)

On the evaporation of dilute droplets in turbulent jets: from physics to applications

F. Picano, J. Wang and F. Dalla Barba
[1] CISAS & Department of Industrial Engineering, University of Padova, Italy.

Despite its importance, evaporation of dilute droplets in turbulent flows still shows many unclear aspects. Indeed, a wide range of turbulent scales and an enormous number of droplets are typically involved, causing the theoretical tackling of the problem to be challenging. In this context, we analized data obtained from point-droplet Eulerian-Lagragian Direct Numerical Simulation (DNS) of turbulent jet-sprays up to a bulk Reynolds number of $Re =$ 10,000. We observe intensive preferential segregation of the dispersed droplets that originates from the entrainment of dry environmental air into the mixing layer and is intensified by small-scale clustering in the far-field region, resulting in a strongly heterogeneous Lagrangian evolution, e.g. Wang et al. (2021). All these aspects contribute to the overall droplet evaporation dynamics which appear much slower than the estimate provided by the d-square law, often used in spray modelling. We attribute this discrepancy to two main reasons: The droplet clustering and the local microscopic droplet thermodynamics, see Dalla Barba et al. (2021). During the talk these aspects will be theoretically discussed in details, together with their implications for applications, such as respiratory flows Wang et al. (2022).

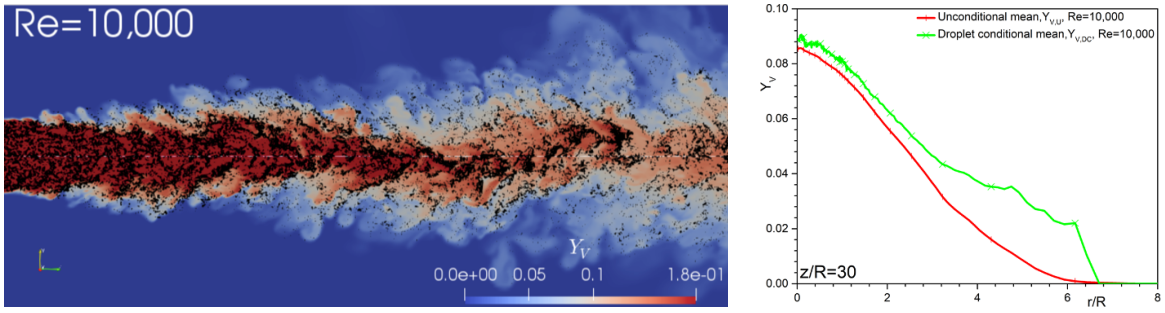

Figure 1: Right: snapshot of the vapour mass fraction Y_v with droplets. Left: Average vapour mass fraction and droplet-conditioned one at the axial distance z/R=30.

References

Wang, J., Dalla Barba, F. and Picano F. *Direct numerical simulation of an evaporating turbulent diluted jet-spray at moderate Reynolds number.* Int. J. Multiphase Flow, 137, 103567, 2021.

Dalla Barba, F., Wang, J. and Picano F. *Revisiting D2-law for the evaporation of dilute droplets* Phys. Fluids, 33, 051701, 2021.

Wang, J., Dalla Barba, F., Roccon, A. Sardina, G., Soldati A. and Picano F. *Modelling the direct virus exposure risk associated with respiratory events.* J. Royal Soc. Interface, 19, 20210819, 2022.

COLLISIONS BETWEEN ICE CRYSTALS IN CLOUDS

M. Z. Sheikh,[1], K. Gustavsson[2], E. Lévêque[3], B. Mehlig[2], A. Pumir[1], and A. Naso[3]
[1]*Laboratoire de Physique, Ecole Normale Supérieure de Lyon and CNRS, Lyon, France*
[2]*Department of Physics, Gothenburg University, Gothenburg, Sweden*
[3]*Laboratoire de MÃl'canique des Fluides et d'Acoustique, CNRS, Ecole Centrale de Lyon, INSA Lyon, and UniversitÃl' Claude Bernard Lyon 1, Lyon, France*

Collisions, resulting in aggregation of ice crystals in clouds, are an important step in the formation of snow aggregates [Fig. 1(a)]. Here, we study the collision process by simulating spheroid-shaped particles settling in turbulent flows, and by determining the probability of collision. We focus on plate-like ice crystals, modelled as oblate spheroids, settling due to gravity in a turbulent flow. These objects are subject to the Stokes force and torque generated by the surrounding fluid. We also take into account the contributions to the drag and torque due to fluid inertia, which are essential to understand the tendency of crystals to settle with their largest dimension oriented horizontally [1].

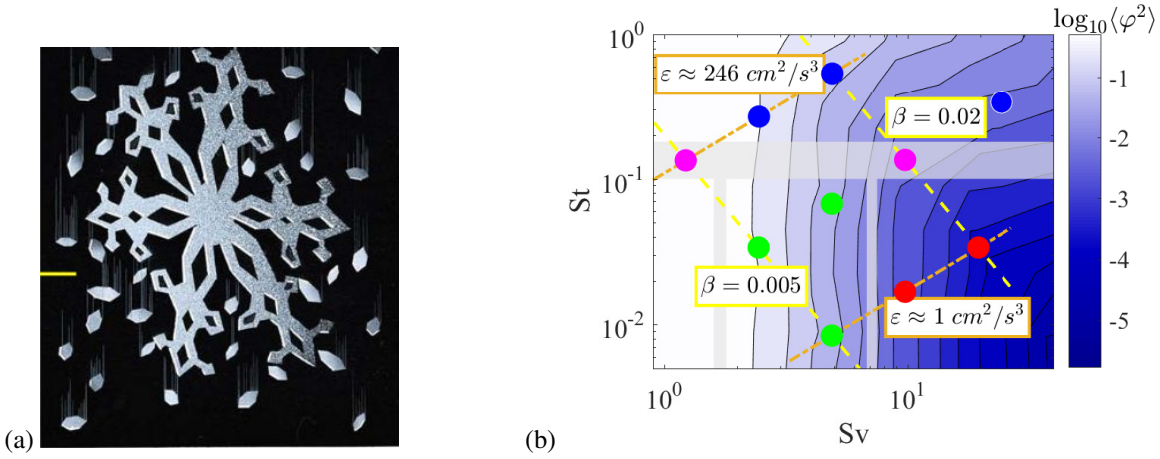

Figure 1. (a) Illustration of the formation of snowflakes due to collisions and aggregation of small ice-crystals (© 2007 Thomson Higher Education). (b) Summary of the collision regimes as a function of the two main parameters of the problem, namely the settling number, Sv (horizontal) and the Stokes number, St (vertical). The yellow dashed lines indicate the constant β-lines, and the orange dashed-dotted lines the constant ε-lines. The color code on the right corresponds to the fluctuations of the angle of orientation φ as a function of $(\mathrm{Sv}, \mathrm{St})$, as discussed in [2]. The points used in the simulation are color coded according to the prevalent physical effect determining the collision: the dominant collision mechanisms are the Saffman-Turner mechanism (red points), the differential settling (green points), and the sling effect (blue points). The two magenta points correspond to transition regimes between several dominant collision mechanisms, which occur in the domains of parameters in transparent gray.

We determine the collision rate between identical crystals [3]. We consider ice crystals of diameter $300\,\mu m$, with aspect ratios in the range $0.005 \leq \beta \leq 0.05$, and over a range of energy dissipation per unit mass, ε, $1\,\mathrm{cm}^2/\mathrm{s}^3 \leq \varepsilon \leq 250\,\mathrm{cm}^2/\mathrm{s}^3$. For all values of β studied, the collision rate increases with the turbulence intensity. The dependence on β is more subtle. Increasing β at low turbulence intensity ($\varepsilon \lesssim 16\,\mathrm{cm}^2/\mathrm{s}^3$) diminishes the collision rate, but increases it at higher $\varepsilon \approx 250\,\mathrm{cm}^2/\mathrm{s}^3$. This complicated dependence is a consequence of the competition between three different physical processes affecting the collision process [see Fig. 1(b)]. First, the velocity gradients in a turbulent flow tend to bring particles together. In addition, differential settling plays a role at small ε when the particles are thin enough (β small), whereas the prevalence of particle inertia at higher ε leads to a strong enhancement of the collision rate.

References

[1] M. Z. Sheikh, K. Gustavsson, D. Lopez, E. Lévêque, B. Mehlig, A. Pumir, and A. Naso, 2020: Importance of fluid inertia for the orientation of spheroids settling in a turbulent flow. *J. Fluid Mech.*, **886**, A9–15.
[2] K. Gustavsson, M. Z. Sheikh, A. Naso, A. Pumir, and B. Mehlig, 2021: Effect of particle inertia on the alignment of small ice crystals in turbulent clouds. *J. Atmos. Sci.*, **78**, 2573–2587.
[3] M. Z. Sheikh, K. Gustavsson, E. Lévêque, B. Mehlig, A. Pumir, and A. Naso, 2021: Colliding ice crystals in turbulent clouds. Submitted to *J. Atmos. Sci.*.

Lagrangian tracking of evaporating droplets in a homogeneous quasi-isotropic turbulence

L. Méès , N. Grosjean, and J. L. Marié
Univ. Lyon, CNRS, Ecole Centrale de Lyon, INSA Lyon, Université Claude Bernard Lyon 1 Laboratoire de Mécanique des Fluides et d'Acoustique, UMR 5509, F-69134, Ecully, France

Turbulence has long been suspected to increase the evaporation rate of droplets via the convective effects it generates. The experimental data reported in this paper provide evidence of this increase and statistically quantify these effects. Ether droplets was released in a quasi-isotropic homogeneous turbulence generated by synthetic jets and tracked by means of Digital Inline Holography. Their Schmidt number is typically of the order of 2 and their Reynolds number is moderate (≤ 3). Their instantaneous positions and diameters have been measured by processing the holograms with an inverse problem approach that has been implemented on a high-performance computer. This allowed us to drastically reduce the processing time and to reconstruct a high number of trajectories for various turbulence conditions. The Lagrangian statistics computed from these trajectories, totaling 1.3 million samples, show that the relative mean motion and turbulence seen by the droplets on average increases their evaporation rate. Within the parameter range investigated, we find that this increase is not well predicted when estimating the convective effect in the Sherwood number with the norm of the instantaneous relative velocity seen by the droplets. In contrast, this increase is very well predicted when the Sherwood number is calculated using a Reynolds number based on the norm of the mean relative velocity plus its root-mean-square fluctuation.

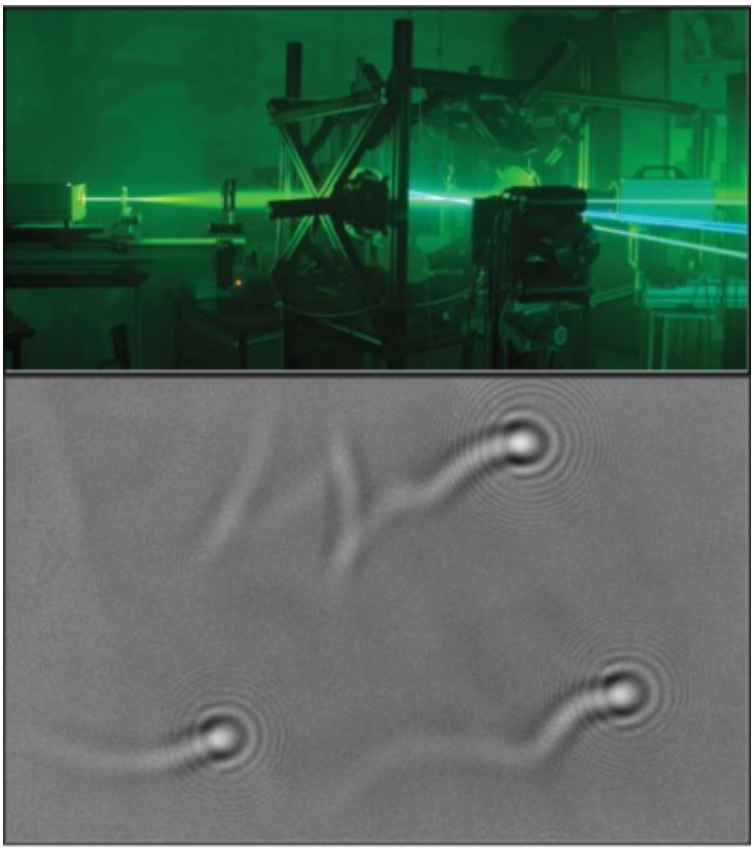

Digital Inline Holography for droplets tracking in turbulence

ERCOFTAC Workshop "Turbulence and Interface" 15-17 June 2022, Ecole Centrale de Lyon

Microphysical time scales and local supersaturation balance at a warm Cloud Top Boundary

Ludovico Fossà,* Shahbozbek Abdunabiev, Mina Golshan, and Daniela Tordella
DISAT, Politecnico di Torino, Italy

Recent results have shown that there is an acceleration in the spread of the size distribution of droplet populations in the region bordering the cloud and undersaturated ambient. We have analyzed the supersaturation balance in this region, which is typically a highly intermittent shearless turbulent mixing layer, under a condition where there is no mean updraft. We have investigated the evolution of the cloud - clear air interface and of the droplets therein via direct numerical simulations. We have compared horizontal averages of the phase relaxation, evaporation, reaction and condensation times within the cloud-clear air interface for the size distributions of the initial monodispersed and polydisperse droplets. For the monodisperse population, a clustering of the values of the reaction, phase and evaporation times, that is around 20-30 seconds, is observed in the central area of the mixing layer, just before the location where the maximum value of the supersaturation turbulent flux occurs. This clustering of values is similar for the polydisperse population but also includes the condensation time. The mismatch between the time derivative of the supersaturation and the condensation term in the interfacial mixing layer is correlated with the planar covariance of the horizontal longitudinal velocity derivatives of the carrier air flow and the supersaturation field, thus suggesting that a quasi-linear relationship may exist between these quantities.

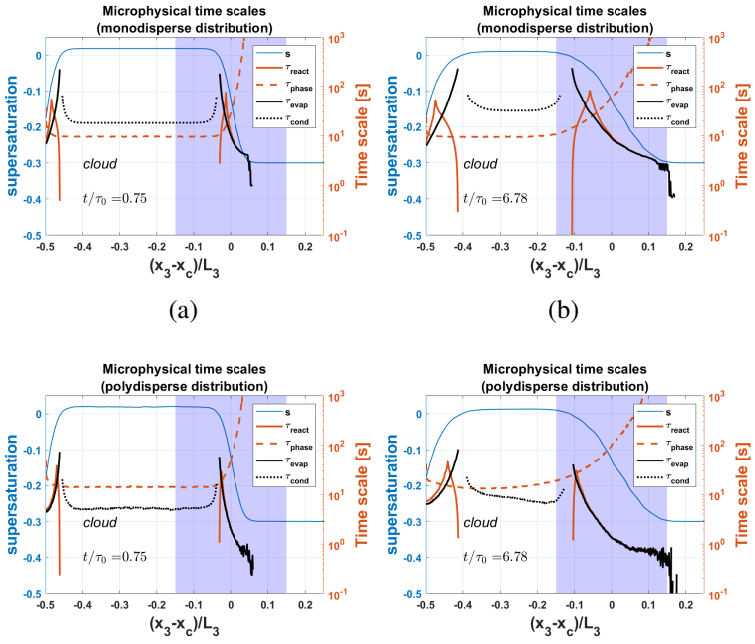

Vertical distribution of the evaporation τ_{evap}, phase relaxation τ_{phase} and reaction τ_{react} time scales computed inside each grid cell and then averaged on horinzontal planes. The data are displayed for the monodisperse, and the polydisperse cases for two different time steps at the beginning and the end of the transient. The planar average of supersaturation $\overline{S}$ is also plotted for comparison purposes.

* Present address: Department of Mechanical Engineering, The University of Sheffield, S1 3JD Sheffield, United Kingdom.

REF: M. Golshan et al., Intermittency acceleration of water droplet population dynamics inside the interfacial layer between cloudy and clear air environments, *International Journal of Multiphase Flow*, 0301-9322, 103669 (2021)